

Supporting Information

for

Chalcogen Atoms Modulated Persistent Room-Temperature Phosphorescence through Intramolecular Electronic Coupling

Letian Xu,^a Guoping Li,^a Tao Xu,^b Weidong Zhang,^a Sikun Zhang,^a Shiwei Yin,^b Zhongfu An,^c and Gang He^{*ab}

^aFrontier Institute of Science and Technology, State Key Laboratory for Strength and Vibration of Mechanical Structures, Xi'an Jiaotong University, Xi'an, Shaanxi province, 710054 (China). E-mail: ganghe@mail.xjtu.edu.cn (G. He)

^bKey Laboratory of Applied Surface and Colloid Chemistry of Ministry of Education, School of Chemistry & Chemical Engineering, Shaanxi Normal University, Xi'an, Shaanxi province, 710062 (China).

^cKey Laboratory of Flexible Electronics (KLOFE) & Institute of Advanced Materials (IAM), Nanjing Tech University, Nanjing, Jiangsu province, 211800 (China).

Contents

1. Materials and instrumentation	S3
2. Synthetic procedures.....	S4
3. UV-vis, excitation and emission spectra of PEPCz in solution.....	S8
4. Phosphorescence spectra of PEPCz in 2-Me-THF at 77 K	S14
5. PL and pRTP spectra of PEPCz in PMMA film.....	S15
6. XRD patterns of PEPCz (E= O, S, Se)	S16
7. PL and pRTP spectra of PEPCz (E= O, S, Se) in amorphous state.....	S16
8. Lifetime decay profiles and data of PEPCz in crystalline state.....	S18
9. pRTP photographs of PEPCz in crystalline state	S23
10. Time-resolved excitation spectra and pRTP mapping of PSePCz in crystalline state.....	S24
11. pRTP spectra under different excitation wavelength of PSePCz in crystalline state	S25
12. pRTP spectra of PEPCz in the air and argon.....	S26
13. Single-crystal X-ray structure determination	S27
14. Intermolecular interactions of PEPCz (E = O, S, Se) in crystal	S33
15. The distances of the n and π groups of some pRTP molecules in literature.....	S36
16. Computational methods and results.....	S40
17. Color-encryption application	S48
18. SEM of PSePCz aggregates in 50% volume fractions of EtOH in water	S49
19. The pRTP sensing application details	S50
20. The ^1H and ^{13}C NMR spectra of PEPCz in CDCl_3	S52
21. Coordinates of molecular structures	S56
Reference	S64

Experimental Section

1. Materials and instrumentation

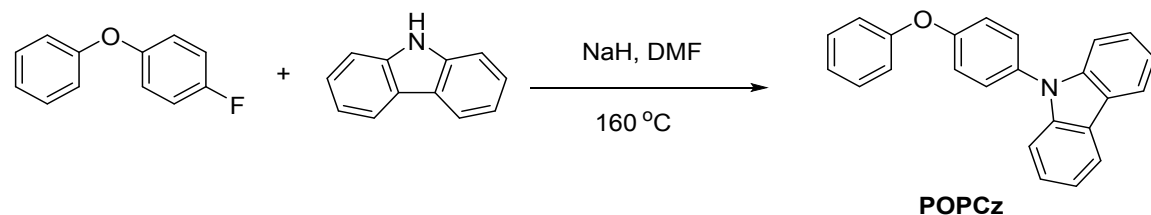
General. THF was freshly distilled under argon from sodium. DMF and EtOH were freshly distilled under argon from calcium hydride. Bromobenzene (98%), 4-fluorophenol (99%), 4-fluorobenzeneboronic acid (98%), potassium tert-butanolate (98%), diphenyl diselenide (97%), diphenyl disulfide (98%), 1-fluoro-4-iodobenzene (98%), potassium hydroxide (98%), copper (99%), copper sulfate pentahydrate (98%), sodium borohydride (98%), tellurium (99%), carbazole (97%) were purchased from Energy Chemical Inc. 1,10-Phenanthroline (99%) purchased from Acros. 1-fluoro-4-phenoxybenzene,¹ 4-fluorophenyl phenyl sulfide,² 4-fluorophenyl phenyl selenide,² 4-fluorophenyl phenyl telluride,² phenyl magnesium bromide,³ diphenyl ditelluride³ were prepared according to literature procedures. If no other special indicated, other reagents and solvents were used as commercially available without further purification. Column chromatographic purification of products was accomplished using 200-300 mesh silica gel.

NMR spectra were measured on a Bruker Avance-400 spectrometer in the solvents indicated; chemical shifts are reported in units (ppm) by assigning TMS resonance in the ¹H spectrum as 0.00 ppm, CDCl₃ resonance in the ¹³C spectrum as 77.0 ppm. Coupling constants are reported in Hz with multiplicities denoted as s (singlet), d (doublet), t (triplet), q (quartet) and m (multiplet). UV-vis measurements were performed using DH-2000-BAL Scan spectrophotometer. Steady-state phosphorescence spectra and excitation spectra were measured using Hitachi F-4600. The photoluminescence quantum efficiency, time-resolved emission spectra and lifetime were obtained using Edinburgh FLSP980 fluorescence spectrophotometer equipped with a xenon lamp (Xe900), a picosecond pulsed laser (EPL-375), a microsecond flash-lamp (μ F900) and an integrating sphere, respectively. Single crystal X-ray diffraction analysis was carried out on a Bruker apex duo equipment. Elemental analysis was conducted using a Euro vector EA3000 Analyzer. High-resolution mass spectra (HRMS) were collected on a Bruker maxis UHR-TOF mass

spectrometer in an ESI positive mode. Powder X-ray diffraction patterns were recorded on a Bruker-D8 Advanced X-ray diffractometer with Cu K α radiation. The **PSePCz** aggregates in EtOH-water mixture were prepared using a typical method: the **PSePCz** (7 mg) was dispersed into water (5 ml), then EtOH (5 ml) was added rapidly with stirring. To accelerate the aggregation, the suspension was sonicated 10 min. The resulting suspension was kept at room temperature and used for sensing applications and SEM measurements. The luminescent photos were taken by a Nikon D5100 camera under the irradiation of hand-held UV lamp at room temperature.

2. Synthetic procedures

Synthesis of 9-(4-phenoxyphenyl)-9H-carbazole (POPCz).



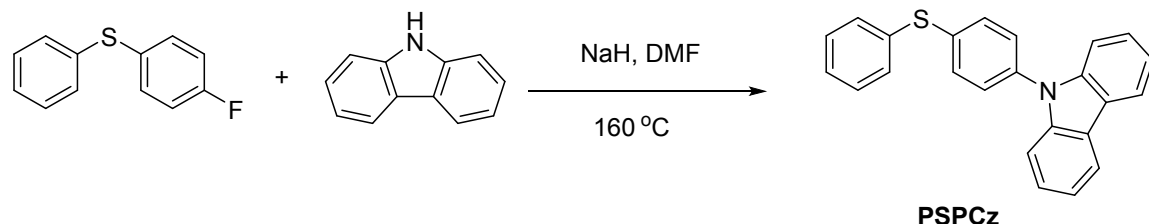
To a solution of sodium hydride (0.51 g, 21.25 mmol) in dry DMF (15 mL) at room temperature was added a solution of carbazole (2.13 g, 12.75 mmol) in dry DMF (13 mL). After the reaction mixture was stirred at room temperature for 30 min, 1-fluoro-4-phenoxybenzene (1.60 g, 8.50 mmol) in 10 mL dry DMF was added, and the mixture was stirred at 160 °C overnight. After the mixture was cooled to room temperature, the reaction was quenched with ice water and the precipitate was filtered. The product was purified by column chromatography (PE/DCM=5/1). Yield: 51%. The crystal sample was recrystallization from dichloromethane and hexane.

^1H NMR (400 MHz, CDCl_3): δ 8.14 (d, 2H), 7.49-7.45 (m, 2H), 7.43-7.39 (m, 6H), 7.30-7.26 (m, 2H), 7.21-7.12 (m, 5H); ^{13}C NMR (100 MHz, CDCl_3): δ 156.68, 156.64, 141.08, 132.41, 129.96, 128.60, 125.90, 123.89, 123.20, 120.29, 119.82, 119.55, 119.43, 109.65. HRMS, m/z: [M $^+$] calcd for $\text{C}_{24}\text{H}_{17}\text{NO}$, 335.1310; found, 335.1300; elemental analysis

calcd (%) for C₂₄H₁₇NO: C, 85.94; H, 5.11; N, 4.18; found: C, 85.85; H, 5.10; N, 4.18.

Melt point of POPCz crystal: 122.2 ~ 122.9 °C.

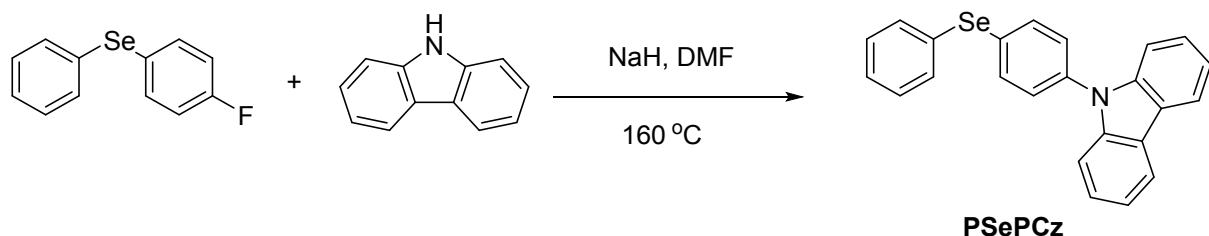
Synthesis of 9-(4-(phenylthio)phenyl)-9*H*-carbazole (PSPCz).



To a solution of sodium hydride (0.57 g, 24.40 mmol) in dry DMF (20 mL) at room temperature was added a solution of carbazole (2.45 g, 14.64 mmol) in dry DMF (15 mL). After the reaction mixture was stirred at room temperature for 30 min, 4-fluorophenyl phenyl sulfide (1.82 g, 9.76 mmol) in 10 mL dry DMF was added, and the mixture was stirred at 160 °C overnight. After the mixture was cooled to room temperature, the reaction was quenched with ice water and the precipitate was filtered. The product was purified by column chromatography (PE/DCM=5/1). Yield: 67%. The crystal sample was recrystallization from dichloromethane and hexane.

¹H NMR (400 MHz, CDCl₃): δ 8.15 (d, 2H), 7.53-7.49 (m, 6H), 7.42-7.39 (m, 6H), 7.38-7.35 (m, 1H), 7.32-7.28 (m, 2H); ¹³C NMR (100 MHz, CDCl₃): δ 140.72, 136.28, 135.78, 134.59, 132.13, 131.37, 129.47, 127.80, 127.65, 125.97, 123.44, 120.32, 120.06, 109.71. HRMS, m/z: [M⁺] calcd for C₂₄H₁₇NS, 351.1082; found, 351.1082; elemental analysis calcd (%) for C₂₄H₁₇NS: C, 82.02; H, 4.88; N, 3.99; S, 9.12; found: C, 82.27; H, 4.96; N, 4.19; S, 8.93. Melt point of PSPCz crystal: 101.3 ~ 101.6 °C.

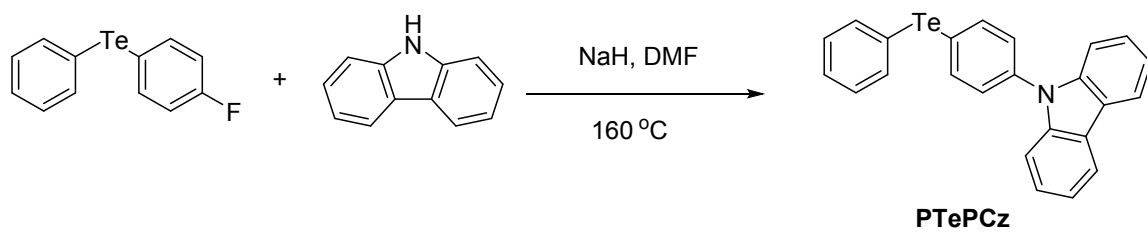
Synthesis of 9-(4-(phenylselanyl)phenyl)-9*H*-carbazole (PSePCz).



To a solution of sodium hydride (0.65 g, 27.00 mmol) in dry DMF (20 mL) at room temperature was added a solution of carbazole (2.71 g, 16.20 mmol) in dry DMF (17 mL). After the reaction mixture was stirred at room temperature for 30 min, 4-fluorophenyl phenyl selenide (2.72 g, 10.80 mmol) in 10 mL dry DMF was added, and the mixture was stirred at 160 °C overnight. After the mixture was cooled to room temperature, the reaction was quenched with ice water and the precipitate was filtered. The product was purified by column chromatography (PE/DCM=5/1) and crystal was obtained through recrystallization from hexane and DCM. Yield: 74%. The crystal sample was recrystallization from dichloromethane and hexane.

¹H NMR (400 MHz, CDCl₃): δ 8.13 (d, 2H), 7.64-7.61 (m, 4H), 7.47-7.45 (m, 2H), 7.41-7.40 (m, 4H), 7.38-7.35 (m, 3H), 7.30-7.26 (m, 2H); ¹³C NMR (100 MHz, CDCl₃): δ 140.63, 136.66, 133.89, 133.51, 130.71, 130.14, 129.58, 127.96, 127.76, 125.96, 123.40, 120.31, 120.04, 109.69. HRMS, m/z: [M⁺] calcd for C₂₄H₁₇NSe, 399.0526; found, 399.0531; elemental analysis calcd (%) for C₂₄H₁₇NSe: C, 72.36; H, 4.30; N, 3.52; found: C, 72.38; H, 4.36; N, 3.50. Melt point of PSePCz crystal: 98.1 ~ 98.3 °C.

Synthesis of 9-(4-(phenyltellanyl)phenyl)-9*H*-carbazole (PTePCz).



To a solution of sodium hydride (0.16 g, 6.75 mmol) in dry DMF (15 mL) at room temperature was added a solution of carbazole (0.68 g, 4.05 mmol) in dry DMF (10 mL). After the reaction mixture was stirred at room temperature for 30 min, 4-fluorophenyl phenyl telluride (0.81 g, 2.70 mmol) in 6 mL dry DMF was added, and the mixture was stirred at 160 °C overnight. After the mixture was cooled to room temperature, the reaction was quenched with ice water and the precipitate was filtered. The product was purified by column chromatography (PE/DCM=5/1) Yield: 56%. The crystal sample was recrystallization from dichloromethane and hexane.

¹H NMR (400 MHz, CDCl₃): δ 8.13 (d, 2H), 7.87-7.84 (m, 4H), 7.43-7.39 (m, 6H), 7.38-7.35 (m, 1H), 7.32-7.26 (m, 4H); ¹³C NMR (100 MHz, CDCl₃): δ 140.58, 138.78, 138.70, 137.32, 129.73, 128.34, 127.92, 125.95, 123.42, 120.31, 120.06, 114.07, 113.60, 109.71. HRMS, m/z: [M⁺] calcd for C₂₄H₁₇NTe, 449.0423; found, 449.0427; elemental analysis calcd (%) for C₂₄H₁₇NTe: C, 64.49; H, 3.83; N, 3.13; found: C, 64.43; H, 4.06; N, 3.36.

Melt point of PTePCz crystal: 66.0 ~ 66.3 °C.

3. UV-vis, excitation and emission spectra of PEPCz in solution

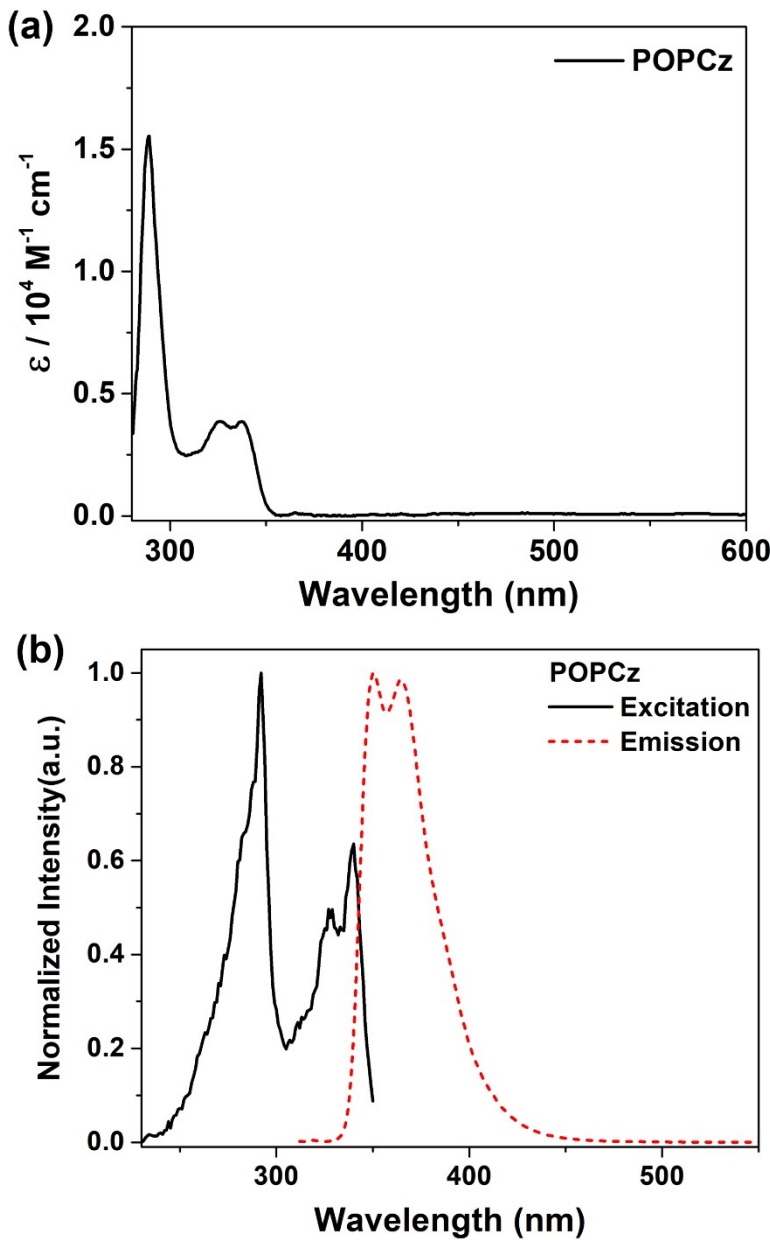


Fig. S1 Photophysical spectra for POPCz in THF. (a) UV-Vis absorbance spectrum; (b) fluorescence excitation (solid line) and emission spectra (dashed line). $[\text{POPCz}] = 3 \times 10^{-5}$ M.

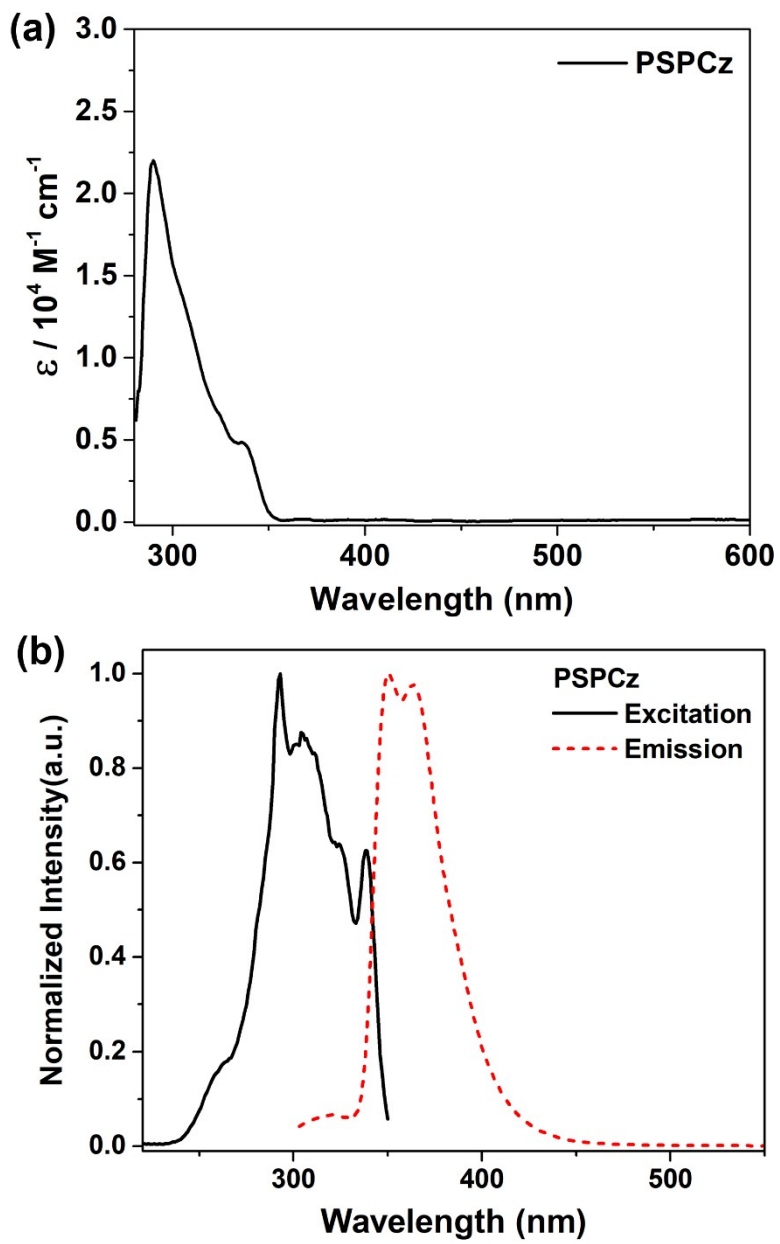


Fig. S2 Photophysical spectra for PSPCz in THF. (a) UV-Vis absorbance spectrum; (b) fluorescence excitation (solid line) and emission spectra (dashed line). $[PSPCz] = 3 \times 10^{-5} M$.

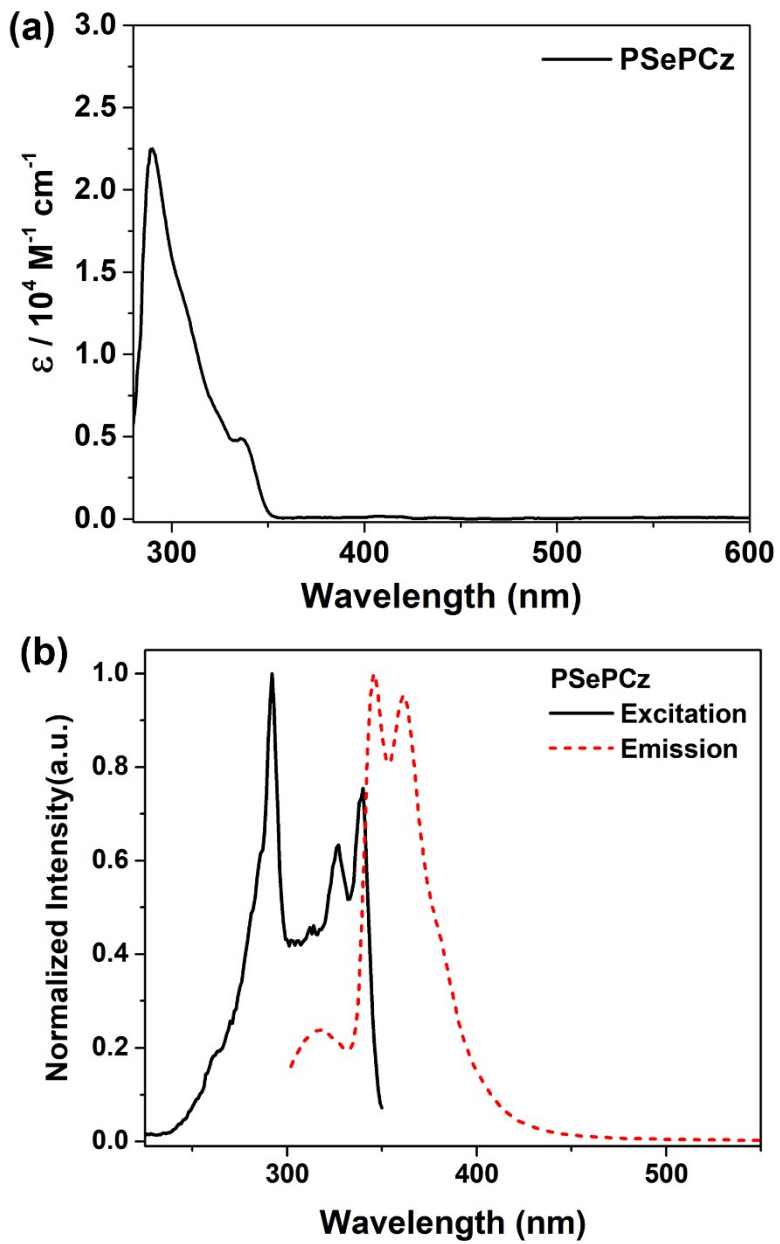


Fig. S3 Photophysical spectra for PSePCz in THF. (a) UV-Vis absorbance spectrum; (b) fluorescence excitation (solid line) and emission spectra (dashed line). $[\text{PSePCz}] = 3 \times 10^{-5}$ M.

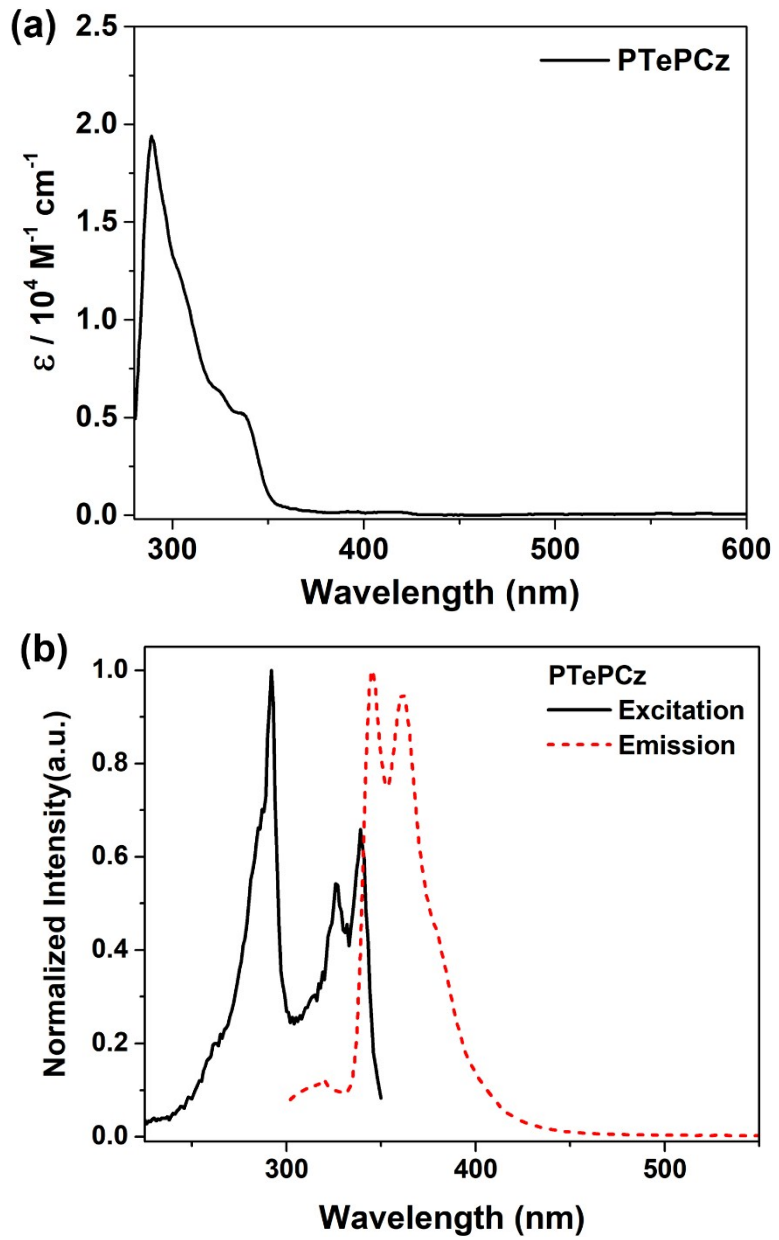


Fig. S4 Photophysical spectra for PTePCz in THF. (a) UV-Vis absorbance spectrum; (b) fluorescence excitation (solid line) and emission spectra (dashed line). $[\text{PTePCz}] = 3 \times 10^{-5} \text{ M}$.

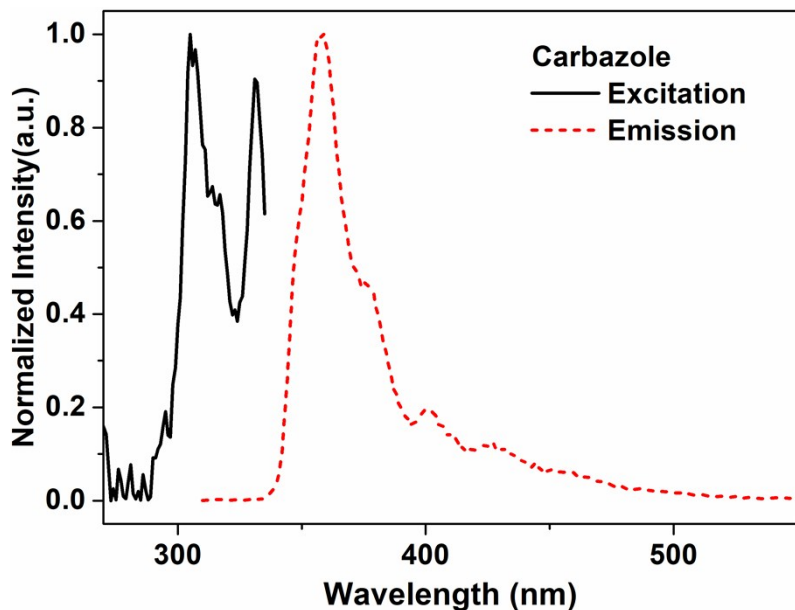


Fig. S5 Photophysical spectra for **Carbazole** in THF. Fluorescence excitation (solid line) and emission spectra (dashed line). [Carbazole] = 3×10^{-5} M.

Table S1. Summarized absorption and emission data of **PEPCz** in solution.

Compound	Absorption			Emission wavelength				
	λ_{ab} (nm)	ϵ [$10^4(M^{-1}cm^{-1})$]	Cyclo exane	Toluene	DCM	THF	Chloroform	MeCN
POPCz	289	1.55	345	350	354	350	353	354
	326	0.39	361	365	366	365	367	365
	337	0.39	--	--	--	--	--	--
PSPCz	290	2.2	345	350	354	350	354	353
	336	0.49	361	365	365	363	365	363
PSePCz	289	2.25	342	348	350	346	351	350
	336	0.49	358	363	365	361	364	363
PTePCz	289	1.94	343	348	349	345	350	350
	337	0.52	359	364	365	361	365	366

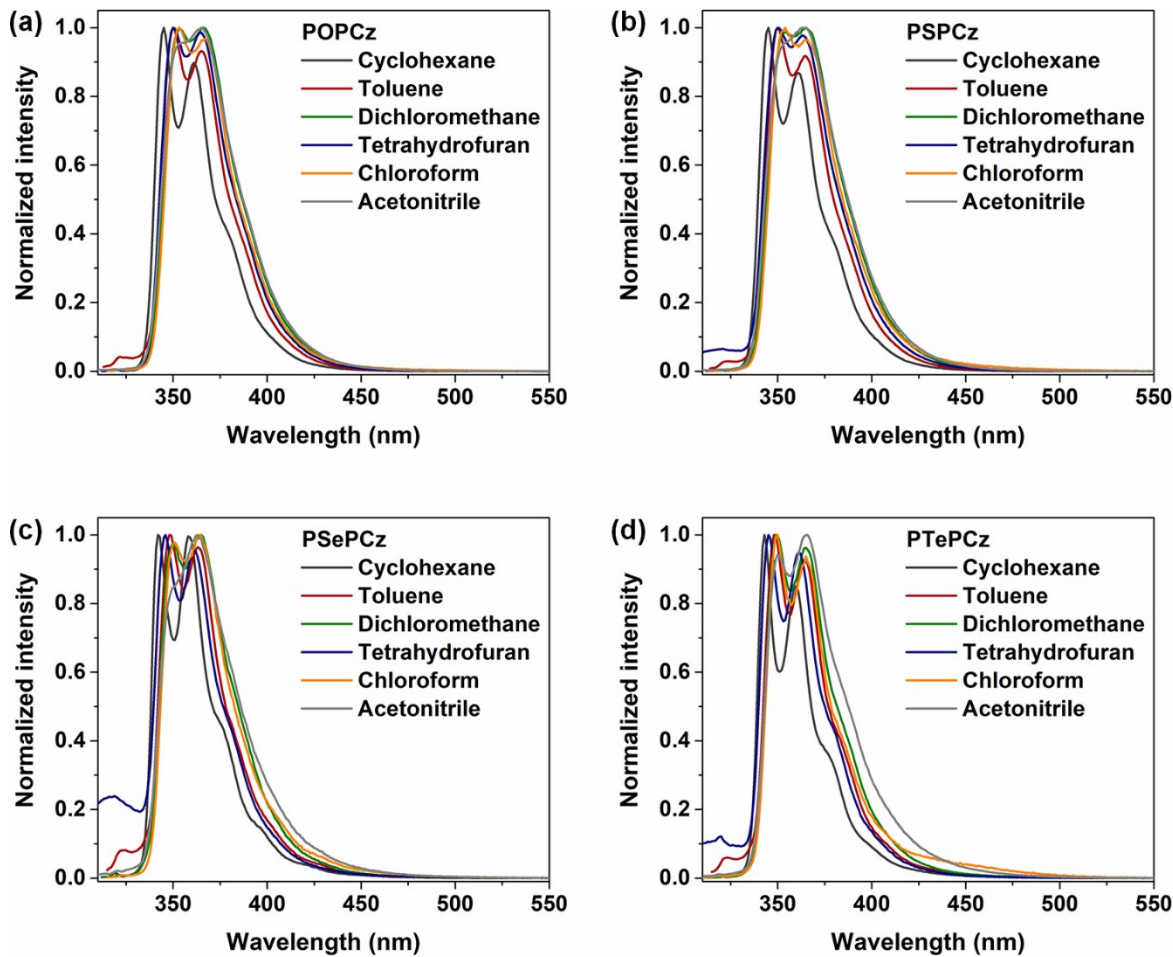


Fig. S6 Photophysical properties of (a) **POPCz**, (b) **PSPCz**, (c) **PSePCz** and (d) **PTePCz** in different solutions. PL spectra of **POPCz**, **PSPCz**, **PSePCz** and **PTePCz** in six types of solvents (cyclohexane, toluene, dichloromethane, tetrahydrofuran, chloroform and acetonitrile) excited at 295 nm at room temperature.

4. Phosphorescence spectra of PEPCz in 2-Me-THF at 77 K

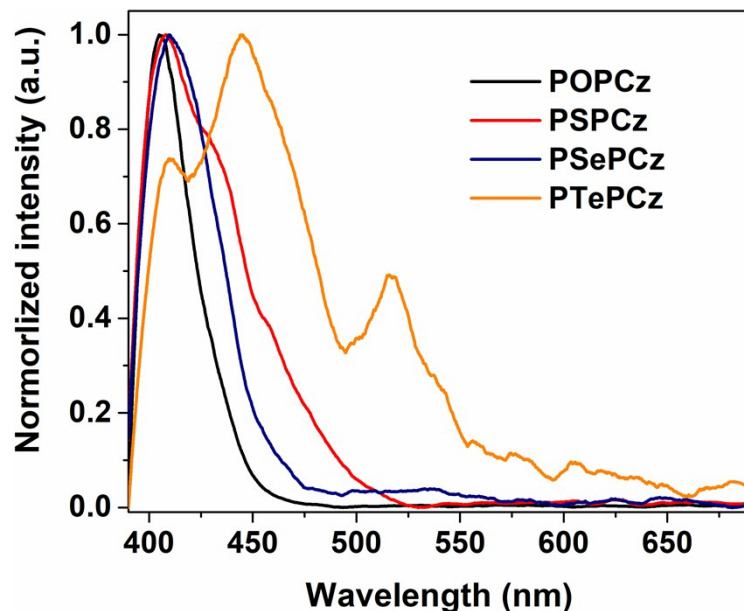


Fig. S7 Phosphorescence spectra of **POPCz**, **PSPCz**, **PSePCz** and **PTePCz** in 2-Me-THF (1.0×10^{-3} M) at 77 K.

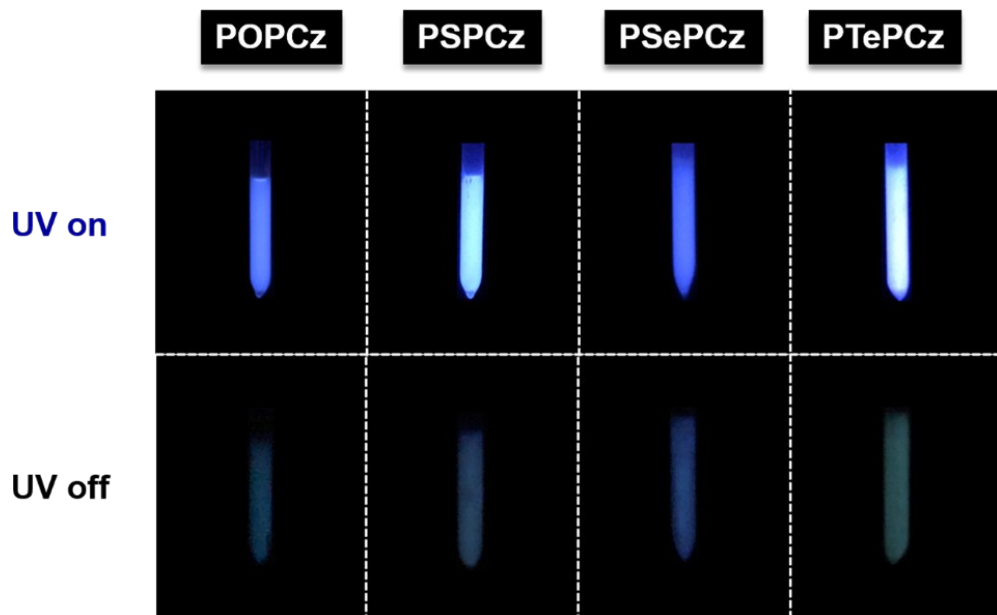


Fig. S8 Photographs of **POPCz**, **PSPCz**, **PSePCz** and **PTePCz** in dilute 2-Me-THF solution (1.0×10^{-3} M) at 77 K before and after excitation light source at 365 nm was switched off.

5. PL and pRTP spectra of PEPCz in PMMA film

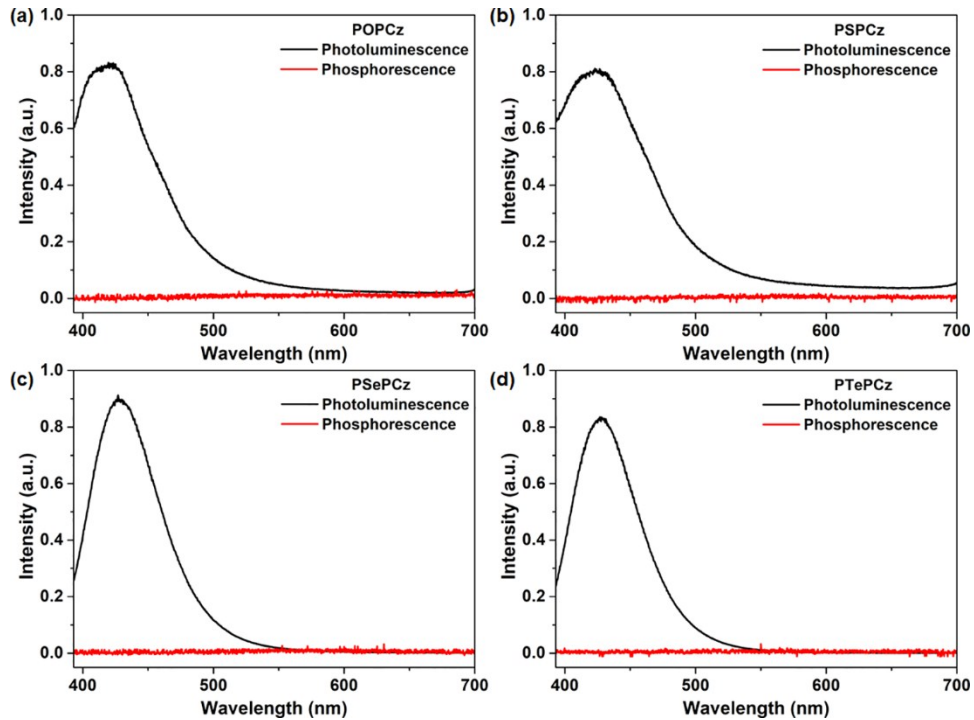


Fig. S9 Photoluminescence and phosphorescence spectra in films of 5 wt% **PEPCz** doped in PMMA under ambient conditions. Excitation wavelength: 365 nm.

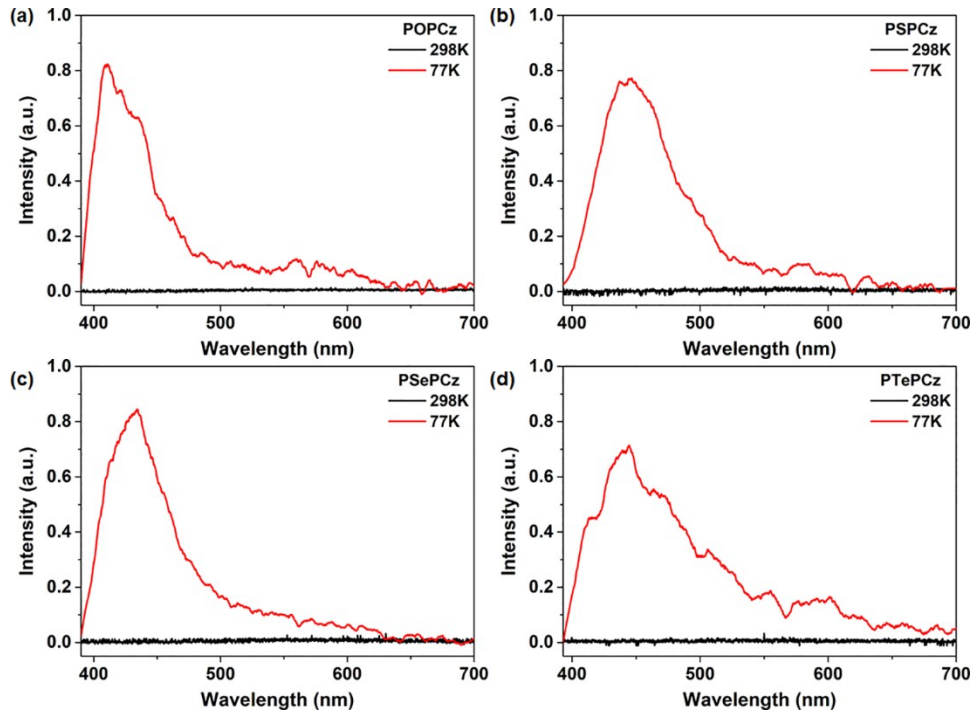


Fig. S10 Phosphorescence spectra in films of 5 wt% **PEPCz** doped in PMMA under air conditions at 298K and 77K. Excitation wavelength: 365 nm.

6. XRD patterns of PEPCz (E= O, S, Se)

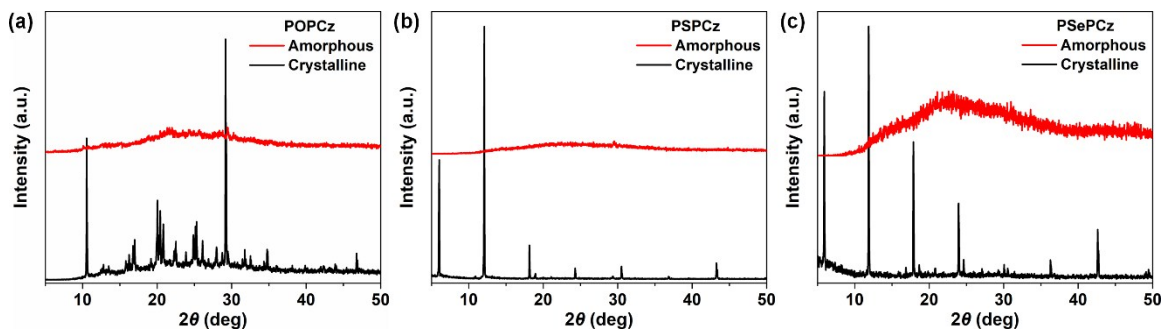


Fig. S11 Powder X-ray diffraction of (a) POPCz, (b) PSPCz and (c) PSePCz crystalline (black line) and amorphous (red line) glass.

7. PL and pRTP spectra of PEPCz (E= O, S, Se) in amorphous state

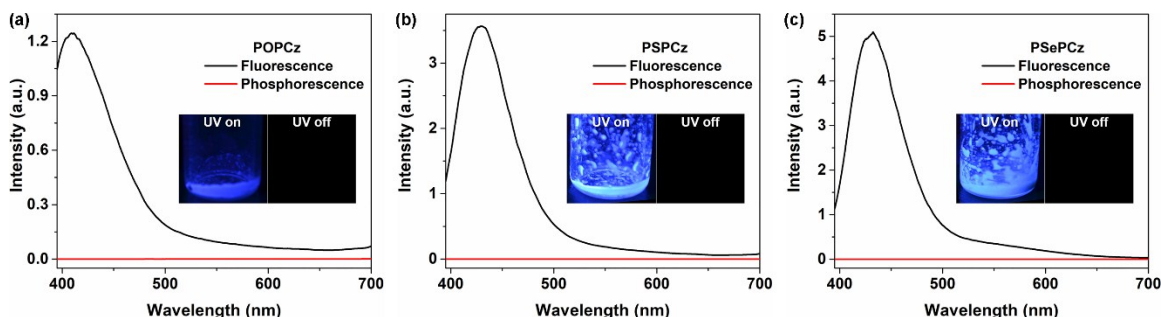


Fig. S12 Steady-state photoluminescence (black line) and phosphorescence spectra (red line) of amorphous (a) POPCz, (b) PSPCz and (c) PSePCz glass at room temperature excited at 365 nm. Inset: Photographs of amorphous POPCz, PSPCz and PSePCz glass at room temperature before and after the irradiation of 365 nm.

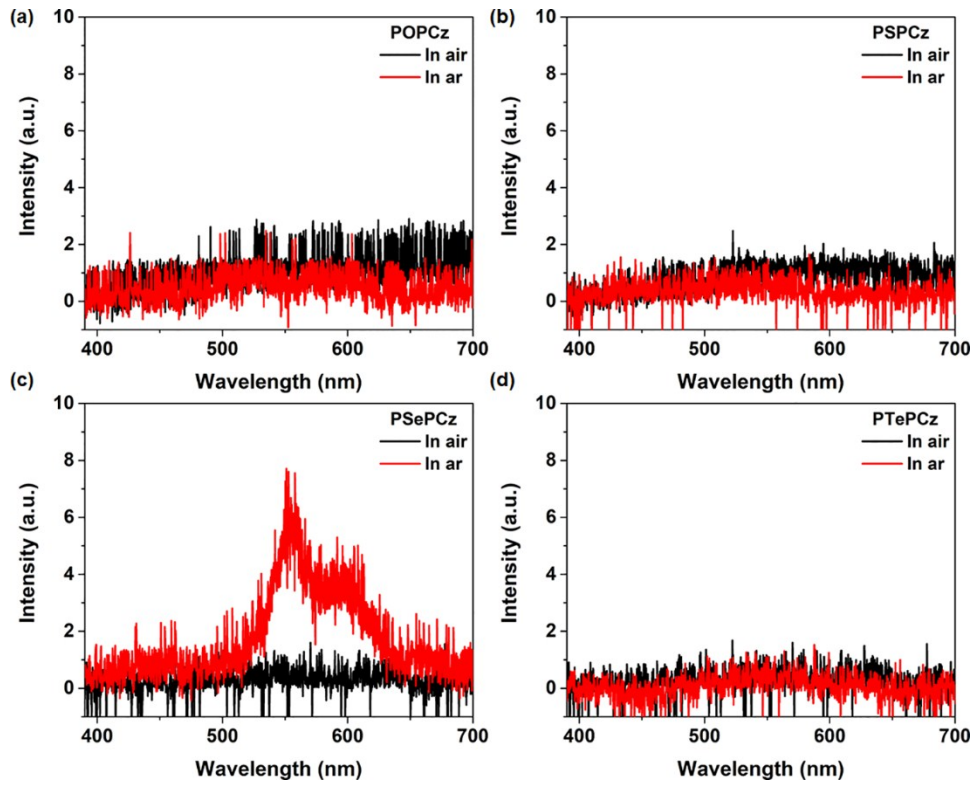


Fig. S13 Phosphorescence spectra of amorphous **PEPCz** at room temperature in air and argon atmosphere respectively. Excitation wavelength: 365 nm.

8. Lifetime decay profiles and data of PEPCz in crystalline state

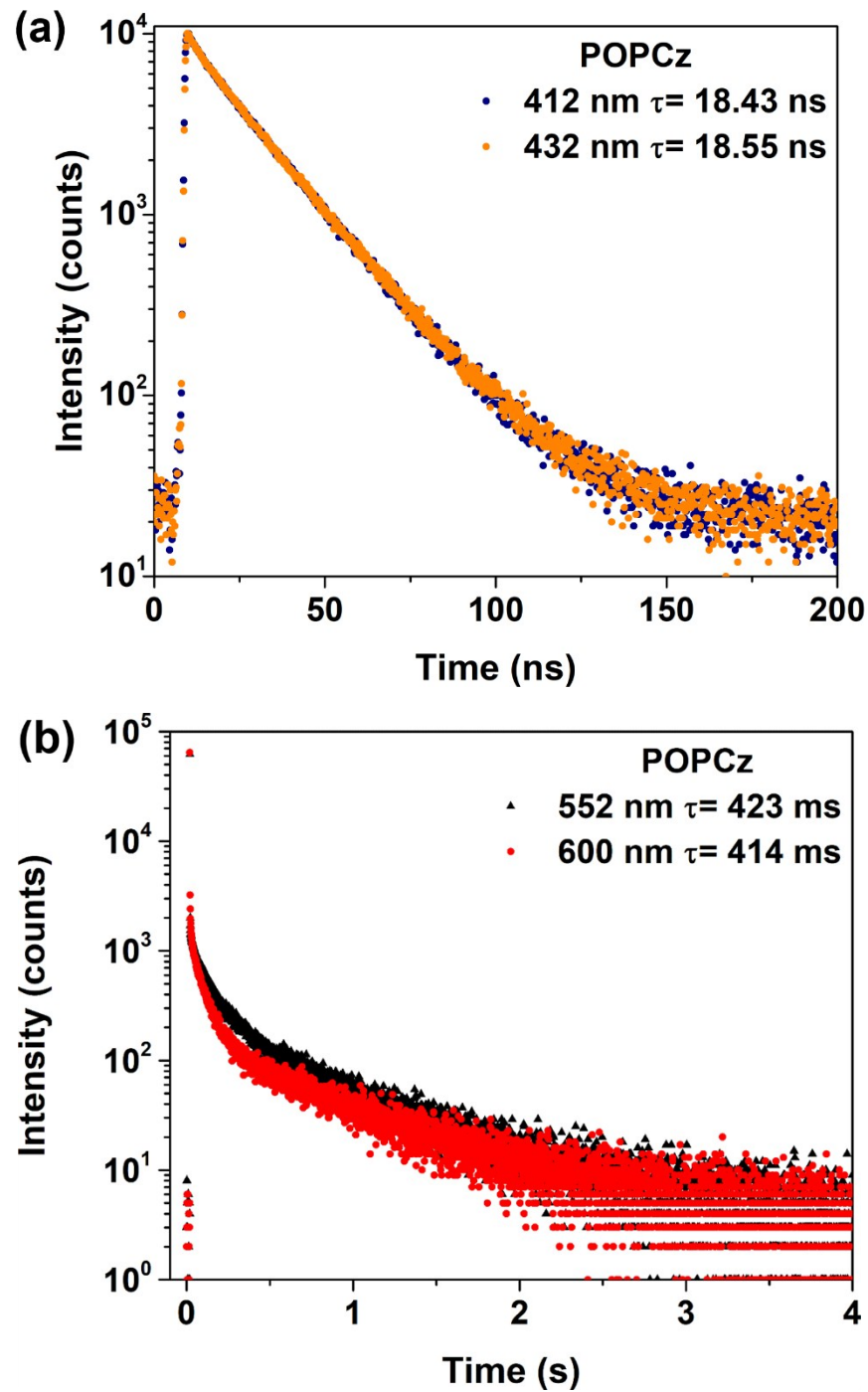


Fig. S14 Lifetime decay profiles of (a) the fluorescence emission bands and (b) the ultralong phosphorescence bands of **POPCz** crystalline powders under ambient conditions.

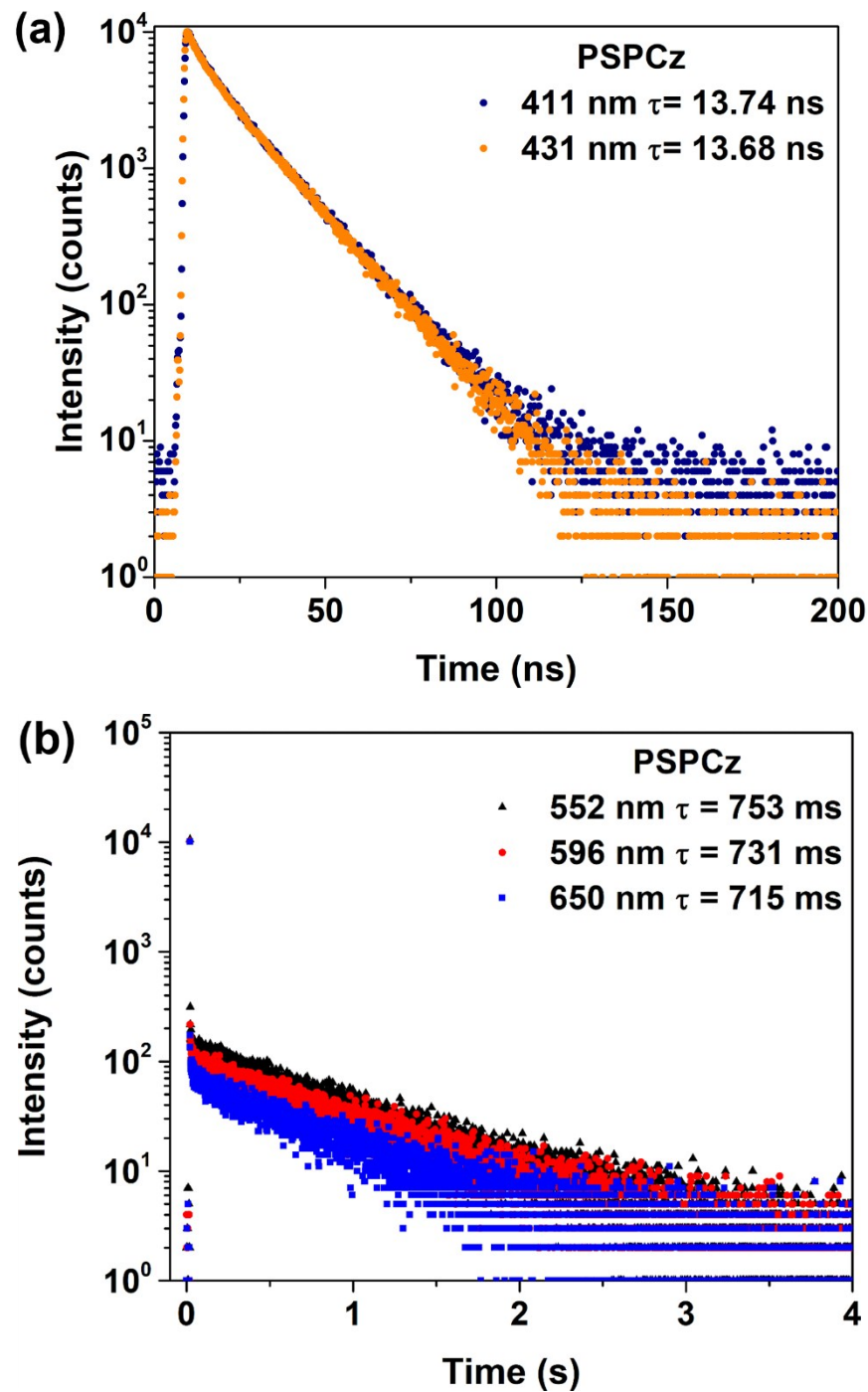


Fig. S15 Lifetime decay profiles of (a) the fluorescence emission bands and (b) the ultralong phosphorescence bands of **PSPCz** crystalline powders under ambient conditions.

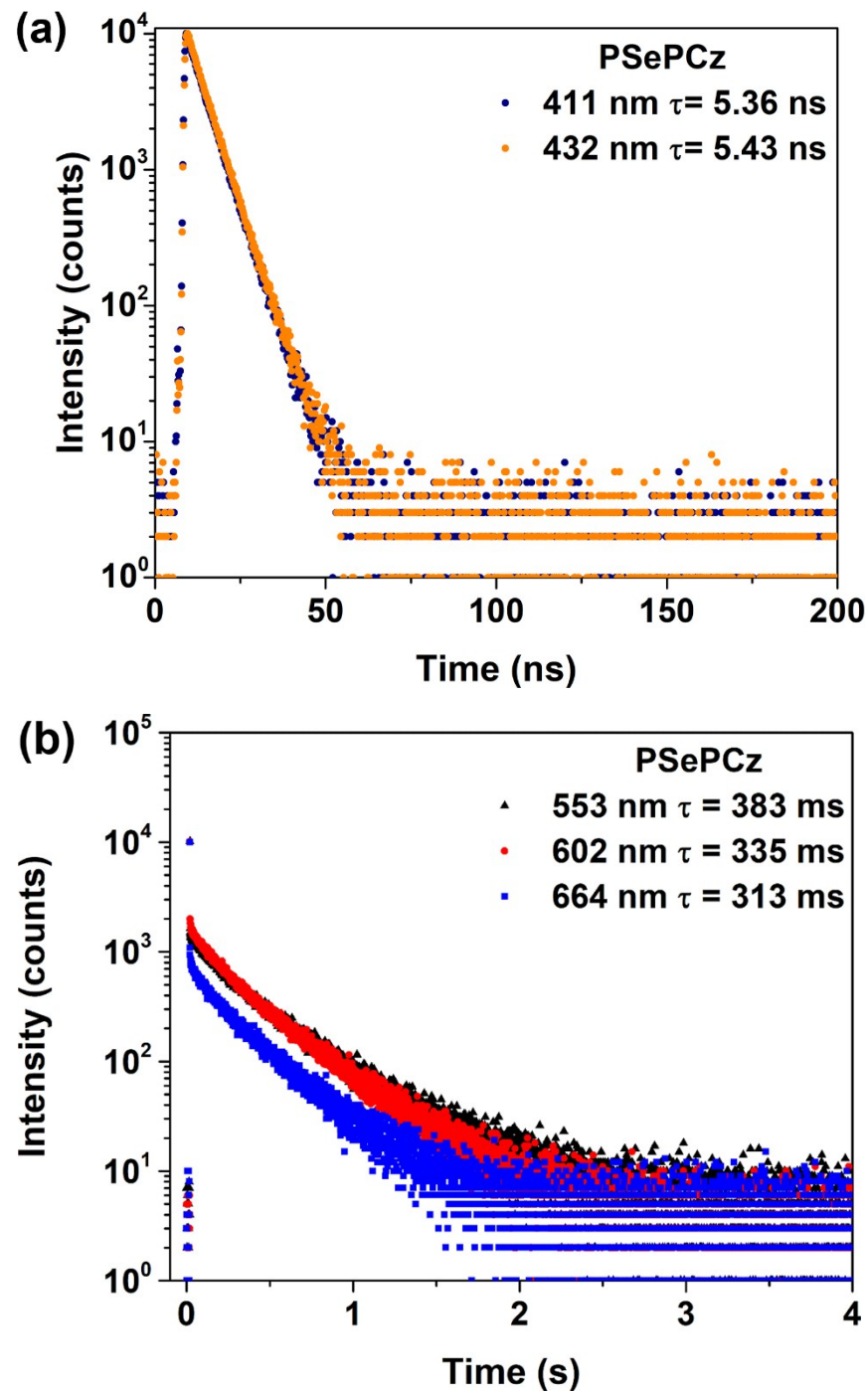


Fig. S16 Lifetime decay profiles of (a) the fluorescence emission bands and (b) the ultralong phosphorescence bands of PSePCz crystalline powders under ambient conditions.

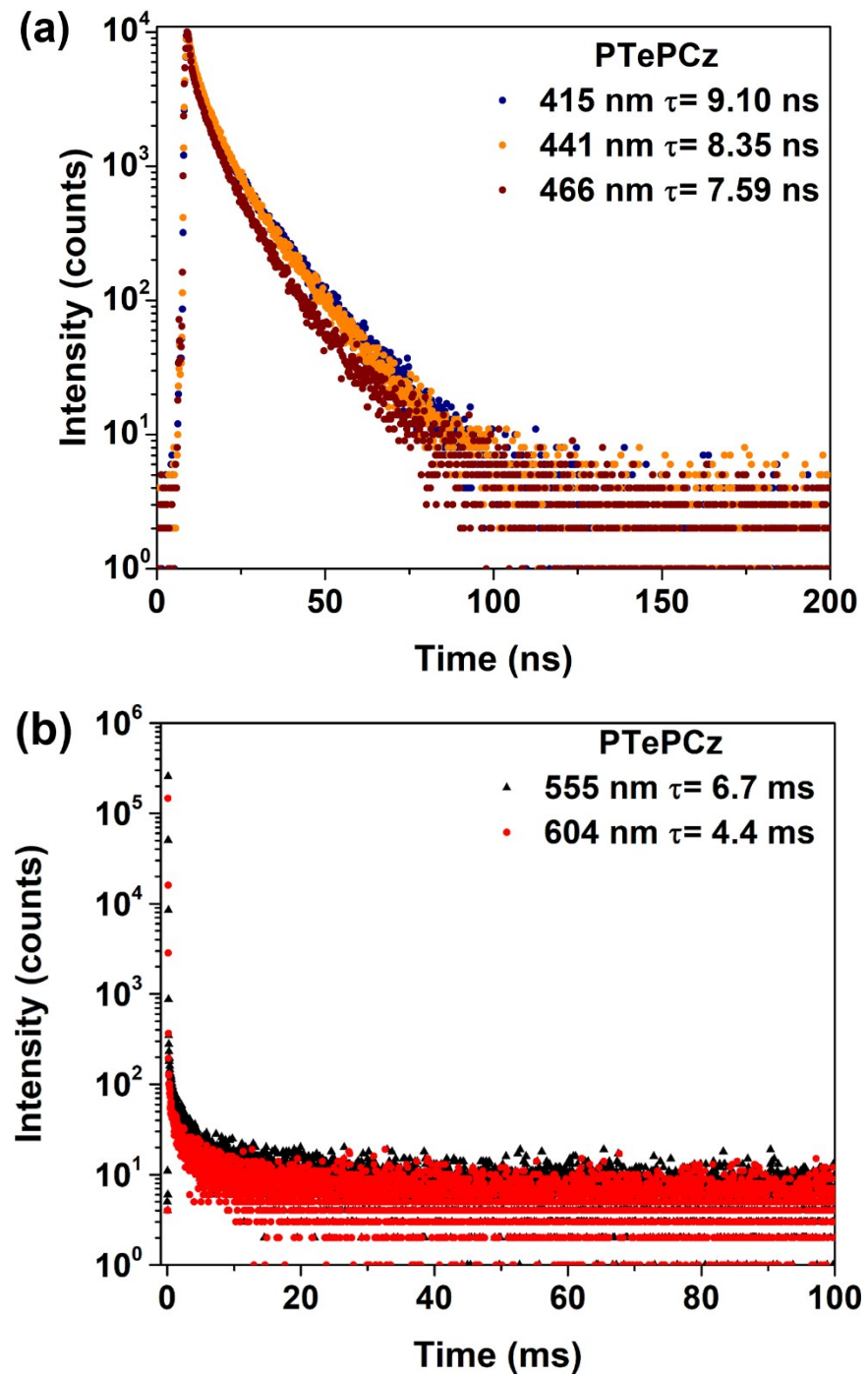


Fig. S17 Lifetime decay profiles of (a) the fluorescence emission bands and (b) the ultralong phosphorescence bands of **PTePCz** crystalline powders under ambient conditions.

Table S2. Photoluminescence lifetimes (τ) of **PEPCz** in crystalline state.

Compound	Wavelength (nm)	Fluorescence				Phosphorescence			
		τ_1 (ns)	A ₁ (%)	τ_2 (ns)	A ₂ (%)	τ_1 (ms)	A ₁ (%)	τ_2 (ms)	A ₂ (%)
POPCz	412	4.43	3.78	18.98	96.22	-	-	-	-
	432	6.40	5.82	19.32	94.18	-	-	-	-
	553	-	-	-	-	94.99	38.12	624.90	61.88
	600	-	-	-	-	64.31	41.74	665.42	58.26
PSPCz	411	4.52	12.26	15.11	87.74	-	-	-	-
	431	4.02	10.74	14.90	89.26	-	-	-	-
	552	-	-	-	-	121.82	3.10	773.70	96.90
	596	-	-	-	-	82.69	3.32	753.17	96.68
	650	-	-	-	-	33.33	2.56	733.36	97.44
PSePCz	411	5.37	100	-	-	-	-	-	-
	432	5.43	100	-	-	-	-	-	-
	553	-	-	-	-	173.56	25.92	456.67	74.08
	602	-	-	-	-	131.71	22.44	394.18	77.56
	664	-	-	-	-	120.13	18.73	357.05	81.27
	415	3.06	33.27	12.61	66.73	-	-	-	-
PTePCz	441	4.02	43.22	12.96	56.78	-	-	-	-
	466	4.12	46.91	12.37	53.09	-	-	-	-
	555	-	-	-	-	0.78	35.11	9.90	64.89
	604	-	-	-	-	0.13	16.46	5.21	83.54

Determined from the fitting function of $I(t) = A_1 e^{-\frac{t}{\tau_1}} + A_2 e^{-\frac{t}{\tau_2}}$ according to the fluorescence and ultralong luminescence decay curves. We hypothesized that the double exponential

fitting of lifetimes were attributed to two kinds of molecular states (i.e., on a surface and inside of a crystal) of PEPCz crystals.

9. pRTP photographs of PEPCz in crystalline state

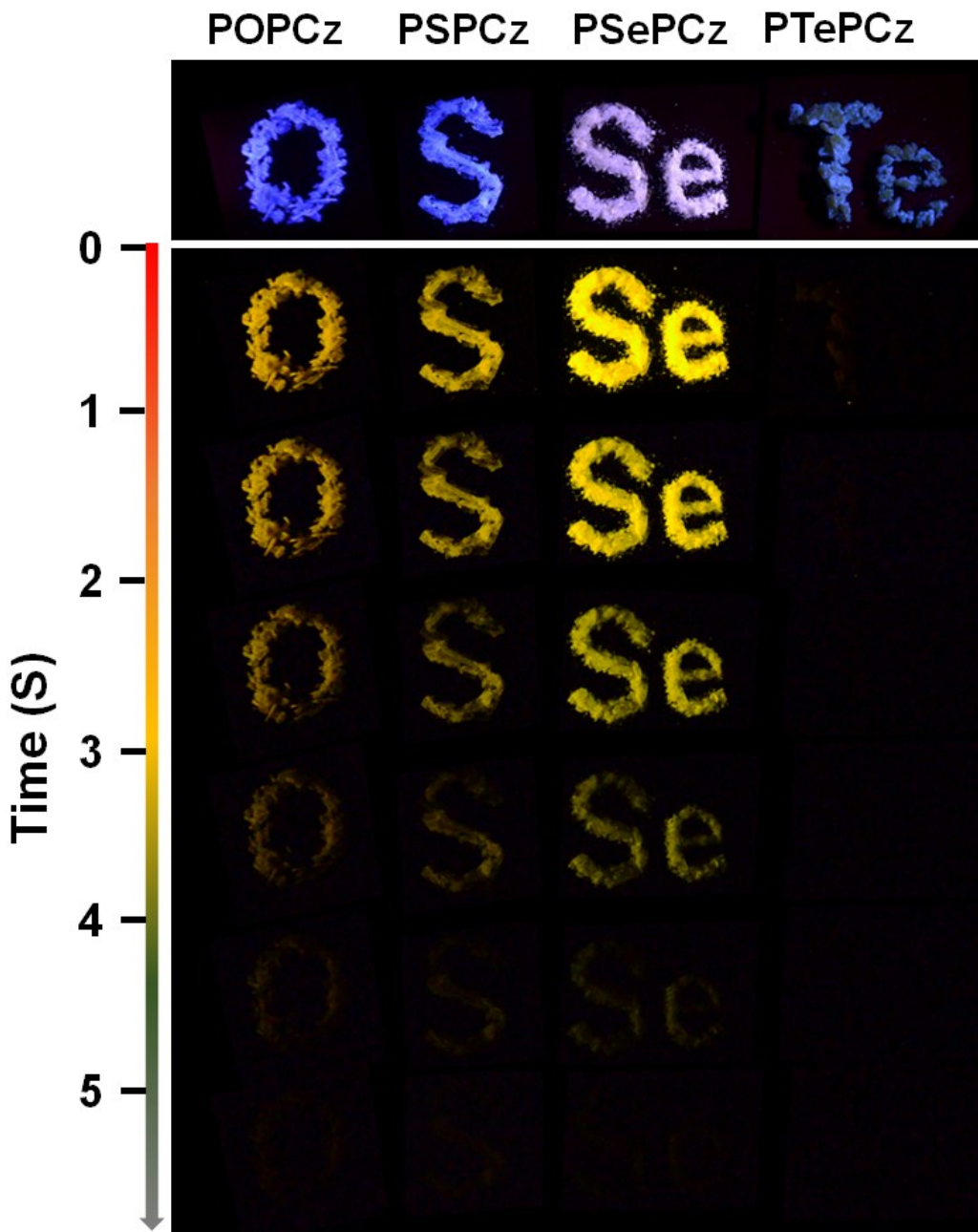


Fig. S18 Photographs of the four pRTP PEPCz materials taken at different time intervals before (first row) and after (succeeding rows) turn-off of the excitation under ambient conditions.

10. Time-resolved excitation spectra and pRTP mapping of PSePCz in crystalline state

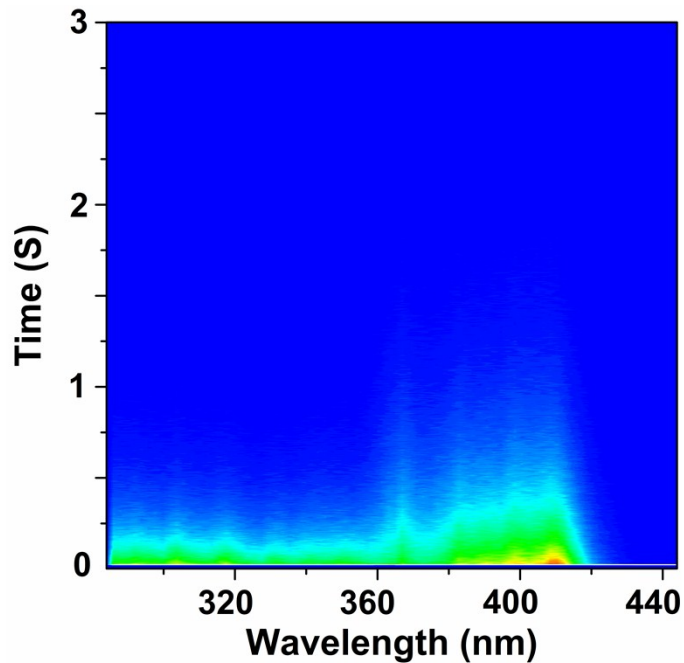


Fig. S19 Time-resolved excitation spectra obtained at 298 K by monitoring the emission of **PSePCz** at 553 nm on varying the excitation wavelengths from 270 to 460 nm.

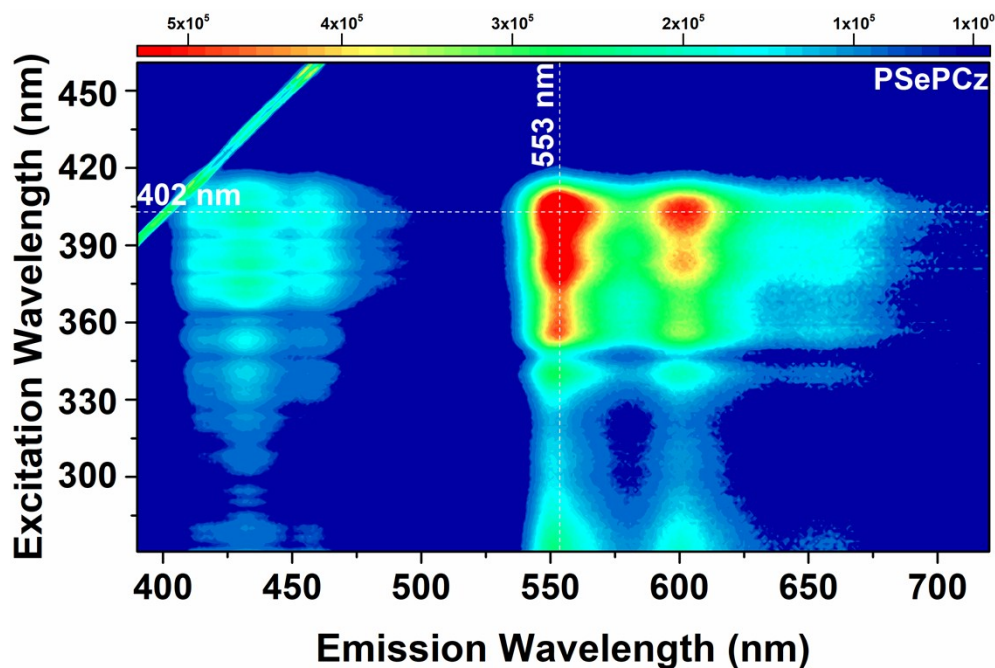


Fig. S20 Excitation-phosphorescence mapping of **PSePCz**.

11. pRTP spectra under different excitation wavelength of PSePCz in crystalline state

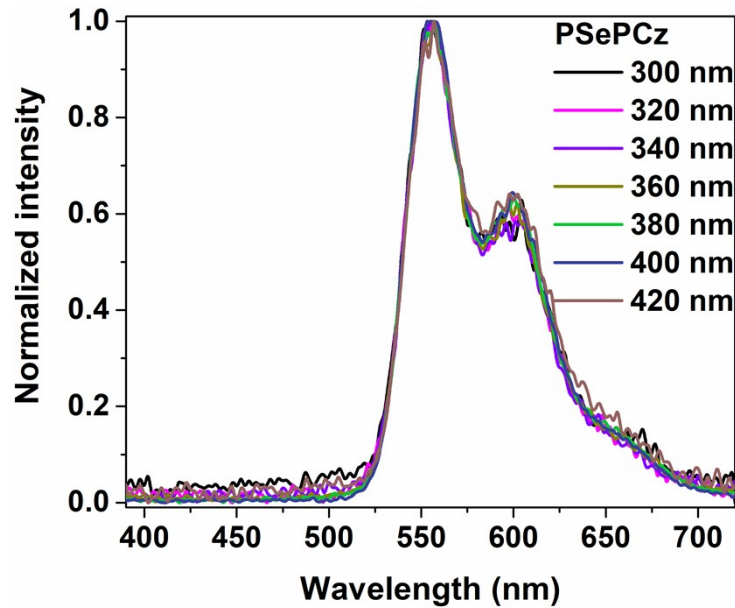


Fig. S21 Phosphorescence spectra of **PSePCz** excited by different wavelength in the crystalline state.

The pRTP emission profiles of **PSePCz** were identical while excitation wavelength changed.

12. pRTP spectra of PEPCz in the air and argon

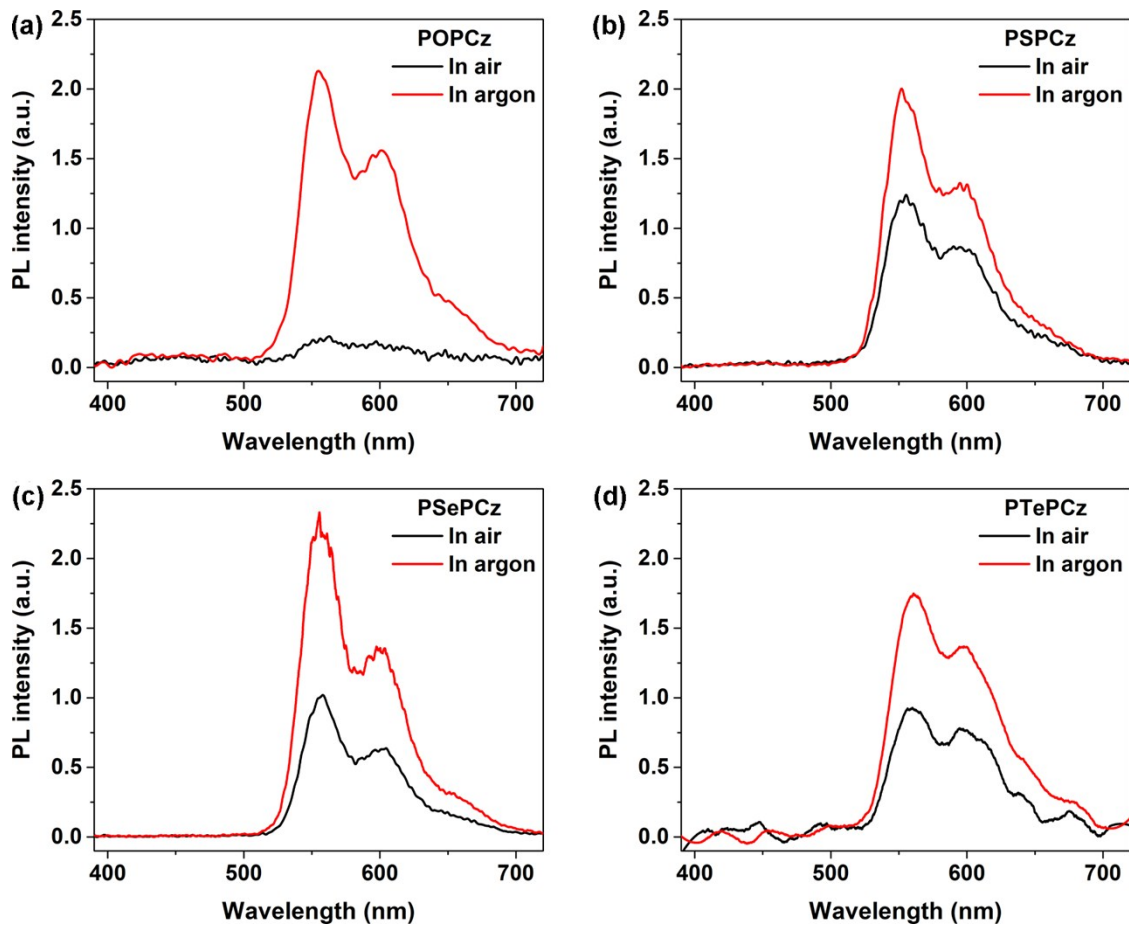


Fig. S22 Phosphorescence spectra at room temperature of **PEPCz** in air and argon atmosphere respectively. Excitation wavelength: 365 nm.

13. Single-crystal X-ray structure determination

X-ray Crystallography. Crystals of appropriate quality for X-ray diffraction studies were selected a suitable crystal, attached to a glass fiber, and quickly placed in a glass vial. All data were collected using a Bruker APEX II CCD detector/D8 diffractometer using Mo/Cu K α radiation. The data were corrected for absorption through Gaussian integration from indexing of the crystal faces. Structures were solved using the direct methods programs SHELXS-97, and refinements were completed using the program SHELXL-97.

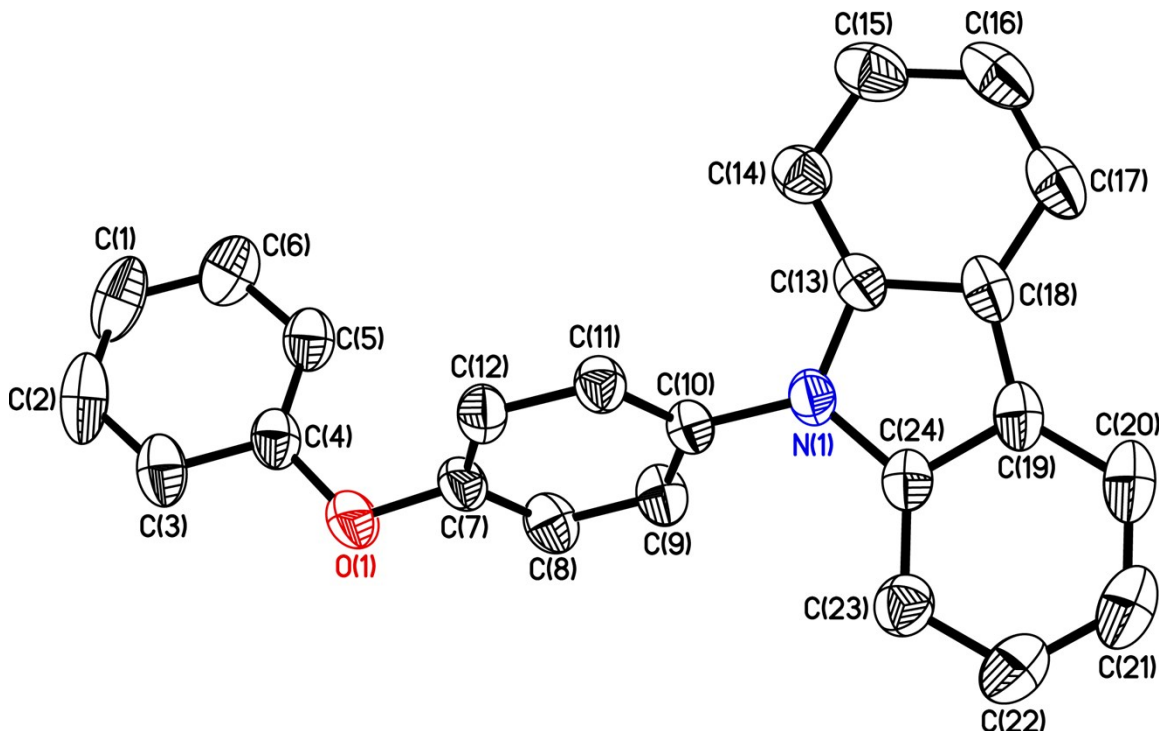


Fig. S23 Molecular Structure of POPCz with thermal ellipsoids presented at a 50% probability level. All hydrogen atoms have been omitted for clarity. Selected bond lengths (\AA): N(1)-C(13), 1.3879(17); N(1)-C(24), 1.3945(18); N(1)-C(10), 1.4221(16); O(1)-C(4), 1.375(2); O(1)-C(7), 1.3875(17). Bond angles (deg): C(13)-N(1)-C(24), 108.53(11); C(13)-N(1)-C(10), 125.93(11); C(24)-N(1)-C(10), 125.34(11); C(4)-O(1)-C(7), 118.82(12); C(5)-C(4)-O(1), 123.08(14); C(3)-C(4)-O(1), 115.68(16).

Table S3. Crystallographic experimental details for compound **POPCz**.

Empirical formula	C ₂₄ H ₁₇ NO
Formula weight	335.38
Temperature	296(2) K
Wavelength	1.54178 Å
Crystal system, space group	Monoclinic, P2 (1) / n
Unit cell dimensions	a = 16.0364(4) Å α = 90 deg. b = 7.5753(2) Å β = 117.2140(10) deg. c = 16.7540(4) Å γ = 90 deg.
Volume	1809.99(8) Å ³
Z, Calculated density	4, 1.231 Mg/m ³
Absorption coefficient	0.585 mm ⁻¹
F(000)	704
Crystal size	? x ? x ? mm
Theta range for data collection	3.161 to 63.785 deg.
Limiting indices	-18<=h<=17, -8<=k<=8, -19<=l<=18
Reflections collected / unique	7314 / 2941 [R(int) = 0.0266]
Completeness to theta = 63.785	98.4 %
Refinement method	Full-matrix least-squares on F ²
Data / restraints / parameters	2941 / 0 / 236
Goodness-of-fit on F ²	1.662
Final R indices [I>2sigma(I)]	R1 = 0.0413, wR2 = 0.1621
R indices (all data)	R1 = 0.0468, wR2 = 0.1737
Extinction coefficient	0.0074(13)
Largest diff. peak and hole	0.200 and -0.197 e. Å ⁻³
CCDC number	1831422

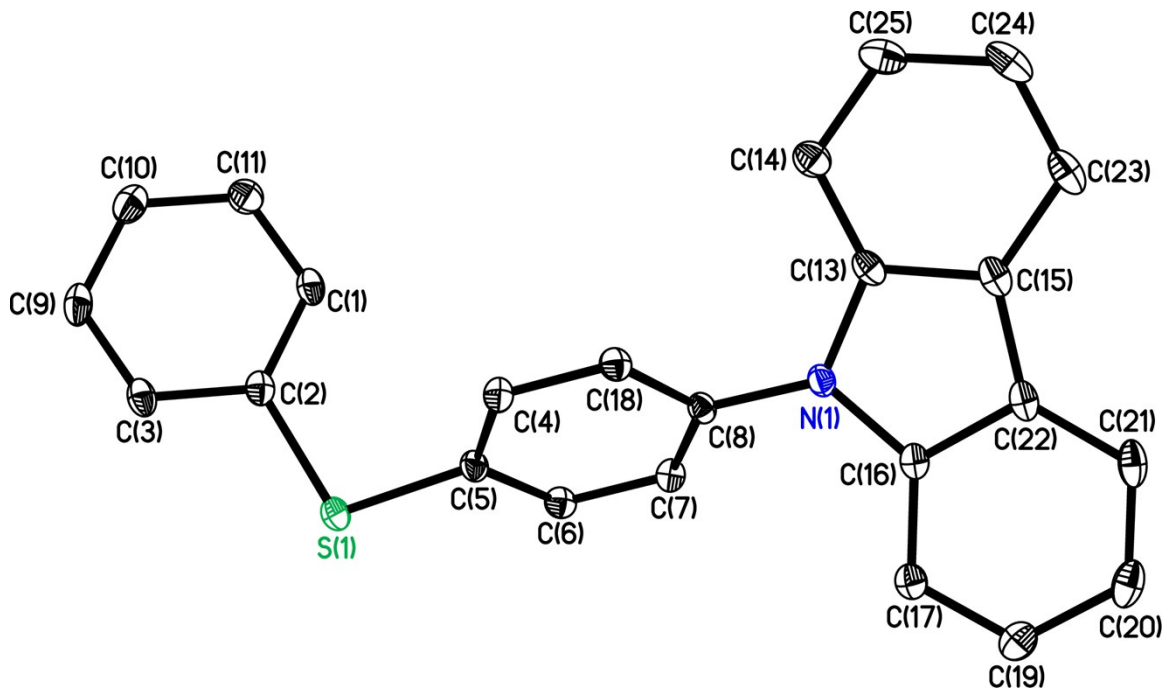


Fig. S24 Molecular Structure of **PSPCz** with thermal ellipsoids presented at a 50% probability level. All hydrogen atoms have been omitted for clarity. Selected bond lengths (\AA): N(1)-C(16), 1.3993(18); N(1)-C(13), 1.3995(18); N(1)-C(8), 1.4176(17); S(1)-C(2), 1.7702(15); S(1)-C(5), 1.7737(14). Bond angles (deg): C(16)-N(1)-C(13), 108.43(11); C(16)-N(1)-C(8), 125.46(11); C(13)-N(1)-C(8), 126.10(12); C(2)-S(1)-C(5), 103.82(7); C(1)-C(2)-S(1), 124.03(11); C(3)-C(2)-S(1), 116.33(11).

Table S4. Crystallographic experimental details for compound **PSPCz**.

Empirical formula	C ₂₄ H ₁₇ NS
Formula weight	351.44
Temperature	153(2) K
Wavelength	0.71073 Å
Crystal system, space group	Monoclinic, P2 (1) / c
Unit cell dimensions	a = 14.7755(6) Å α = 90 deg. b = 16.6199(6) Å β = 100.0350(10) deg. c = 7.5149(3) Å γ = 90 deg.
Volume	1817.18(12) Å ³
Z, Calculated density	4, 1.285 Mg/m ³
Absorption coefficient	0.185 mm ⁻¹
F(000)	736
Crystal size	? x ? x ? mm
Theta range for data collection	2.451 to 27.719 deg.
Limiting indices	-19<=h<=19, -21<=k<=21, -9<=l<=9
Reflections collected / unique	62652 / 4171 [R(int) = 0.0492]
Completeness to theta = 25.242	99.8 %
Refinement method	Full-matrix least-squares on F ²
Data / restraints / parameters	4171 / 0 / 235
Goodness-of-fit on F ²	1.155
Final R indices [I>2sigma(I)]	R1 = 0.0384, wR2 = 0.0978
R indices (all data)	R1 = 0.0513, wR2 = 0.1123
Extinction coefficient	n/a
Largest diff. peak and hole	0.473 and -0.569 e. Å ⁻³
CCDC number	1831423

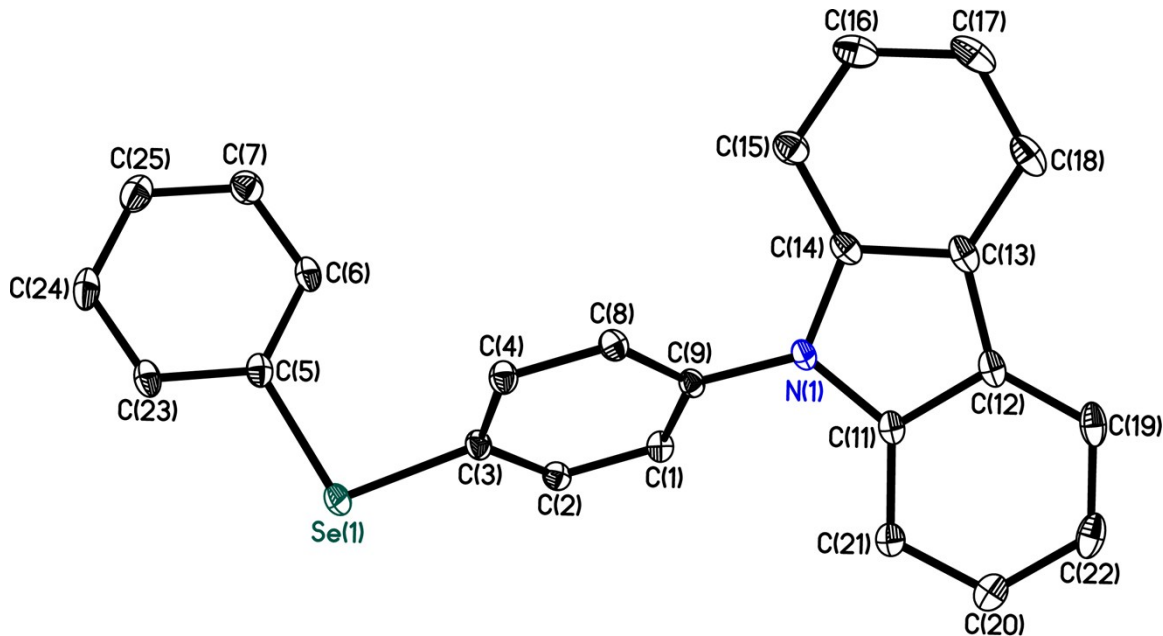
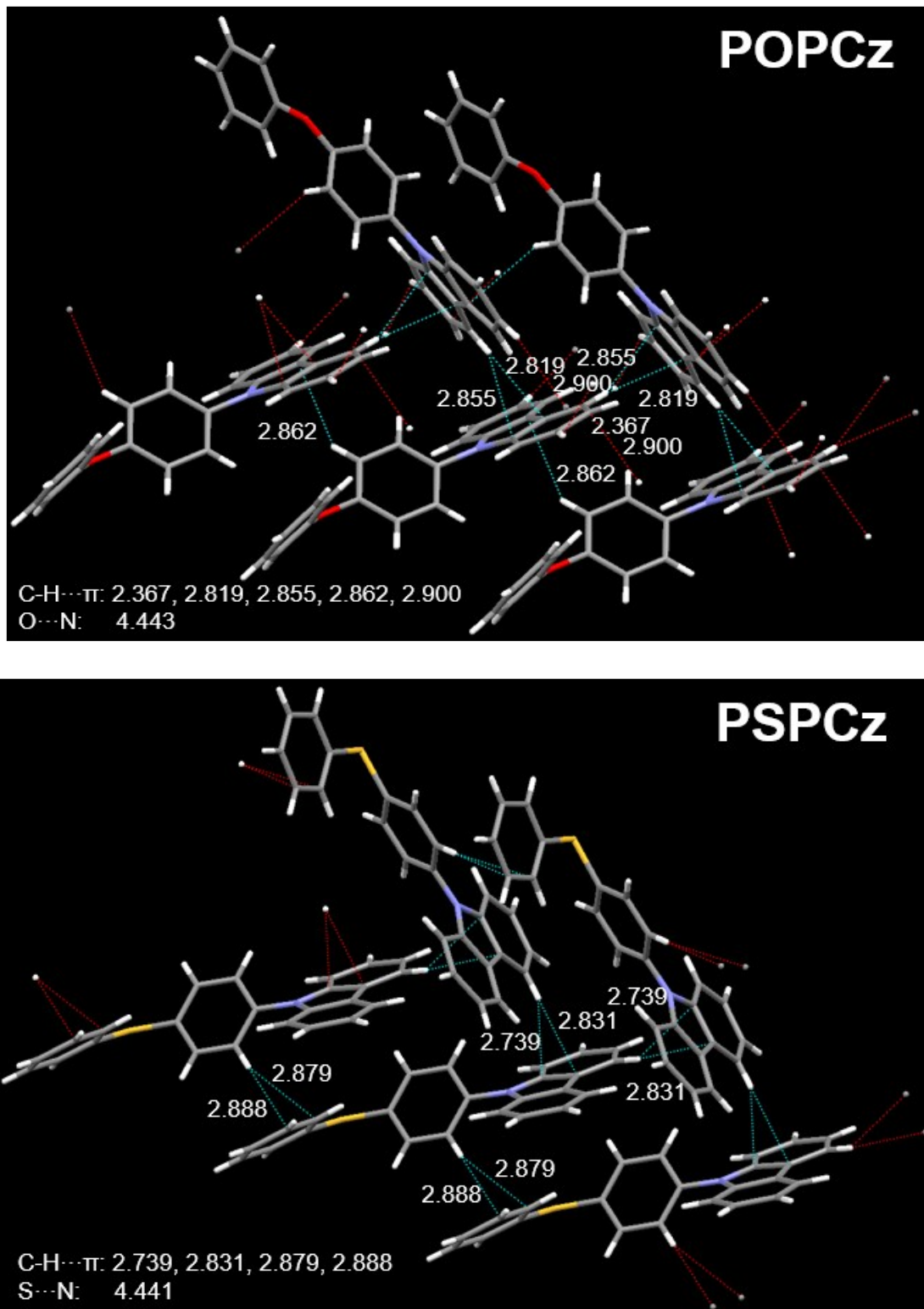


Fig. S25 Molecular Structure of PSePCz with thermal ellipsoids presented at a 50% probability level. All hydrogen atoms have been omitted for clarity. Selected bond lengths (\AA): N(1)-C(11), 1.395(2); N(1)-C(14), 1.399(2); N(1)-C(9), 1.4211(19); Se(1)-C(3), 1.9143(15); Se(1)-C(5), 1.9149(17). Bond angles (deg): C(11)-N(1)-C(14), 108.63(13); C(11)-N(1)-C(9), 125.42(13); C(14)-N(1)-C(9), 125.94(13); C(3)-Se(1)-C(5), 101.09(7); C(2)-C(3)-Se(1), 118.39(11); C(4)-C(3)-Se(1), 121.46(12).

Table S5. Crystallographic experimental details for compound **PSePCz**.

Empirical formula	C ₂₄ H ₁₇ NSe
Formula weight	398.34
Temperature	153(2) K
Wavelength	0.71073 (Å)
Crystal system, space group	Monoclinic, P2(1)/c
Unit cell dimensions	a = 14.9778(5) Å α = 90 deg. b = 16.6273(6) Å β = 99.6790(10) deg. c = 7.5305(2) Å γ = 90 deg.
Volume	1848.70(10) Å ³
Z, Calculated density	4, 1.431 Mg/m ³
Absorption coefficient	2.037 mm ⁻¹
F(000)	808
Crystal size	? x ? x ? mm
Theta range for data collection	2.450 to 27.556 deg.
Limiting indices	-19<=h<=19, -21<=k<=21, -9<=l<=9
Reflections collected / unique	60339 / 4254 [R(int) = 0.0380]
Completeness to theta = 25.242	99.70%
Refinement method	Full-matrix least-squares on F ²
Data / restraints / parameters	4254 / 0 / 235
Goodness-of-fit on F ²	1.118
Final R indices [I>2sigma(I)]	R1 = 0.0259, wR2 = 0.0703
R indices (all data)	R1 = 0.0310, wR2 = 0.0729
Extinction coefficient	n/a
Largest diff. peak and hole	0.431 and -0.684 e. Å ⁻³
CCDC number	1831424

14. Intermolecular interactions of PEPCz (E = O, S, Se) in crystal



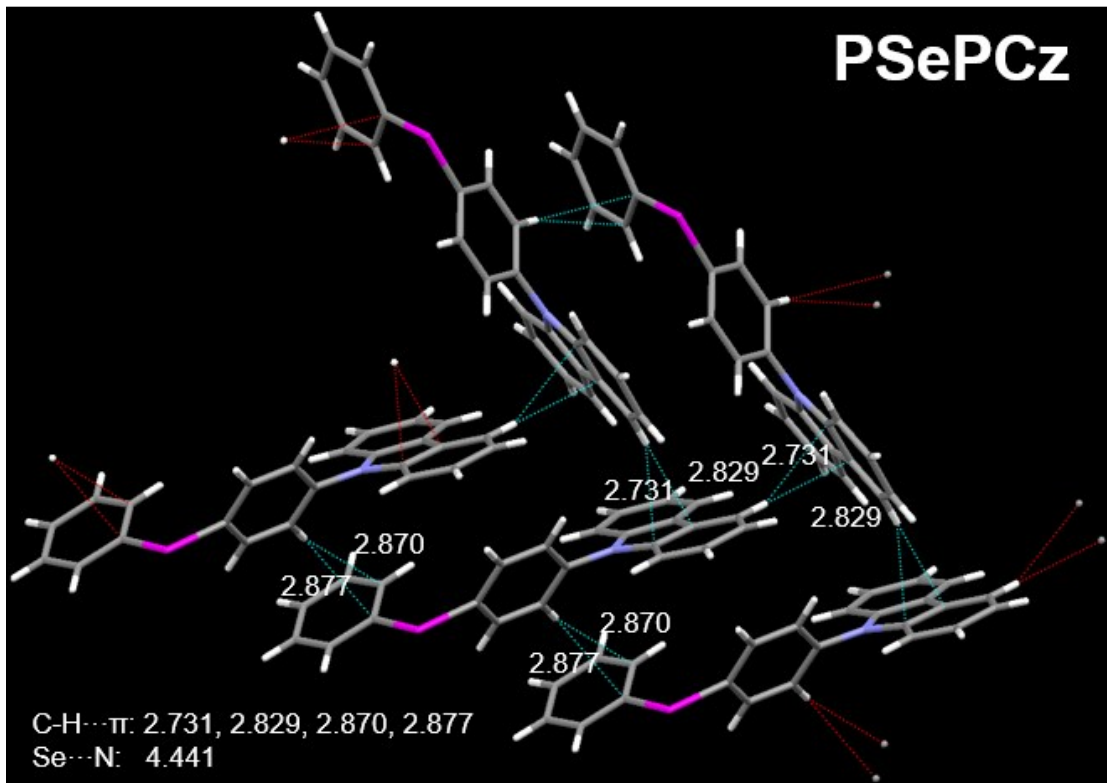


Fig. S26 Single-crystal structure and molecular packing of **POPCz**, **PSPCz**, **PSePCz** with denoted intermolecular interactions. For **POPCz**, C-H···H-C (2.367 Å) and C-H···π (2.900 Å) interactions were observed compared with **PSPCz** and **PSePCz**.

The crystal packing of **POPCz** indicated that the network was constructed by C-H···H-C and C-H···π bonding interactions. In **PSPCz**, the intermolecular interaction C-H···π was shorter than in **POPCz** and there were no C-H···H-C interactions observed. The C-H···π contacts in **PSePCz** crystal network were slightly shorter than in **POPCz** and **PSPCz** (Fig. S26 and S27). These hydrogen bonds provide stabilizing energy for crystal packing and confine molecular geometry, thus, the molecular movement will be largely restricted in the photophysical process between the ground and excited states.

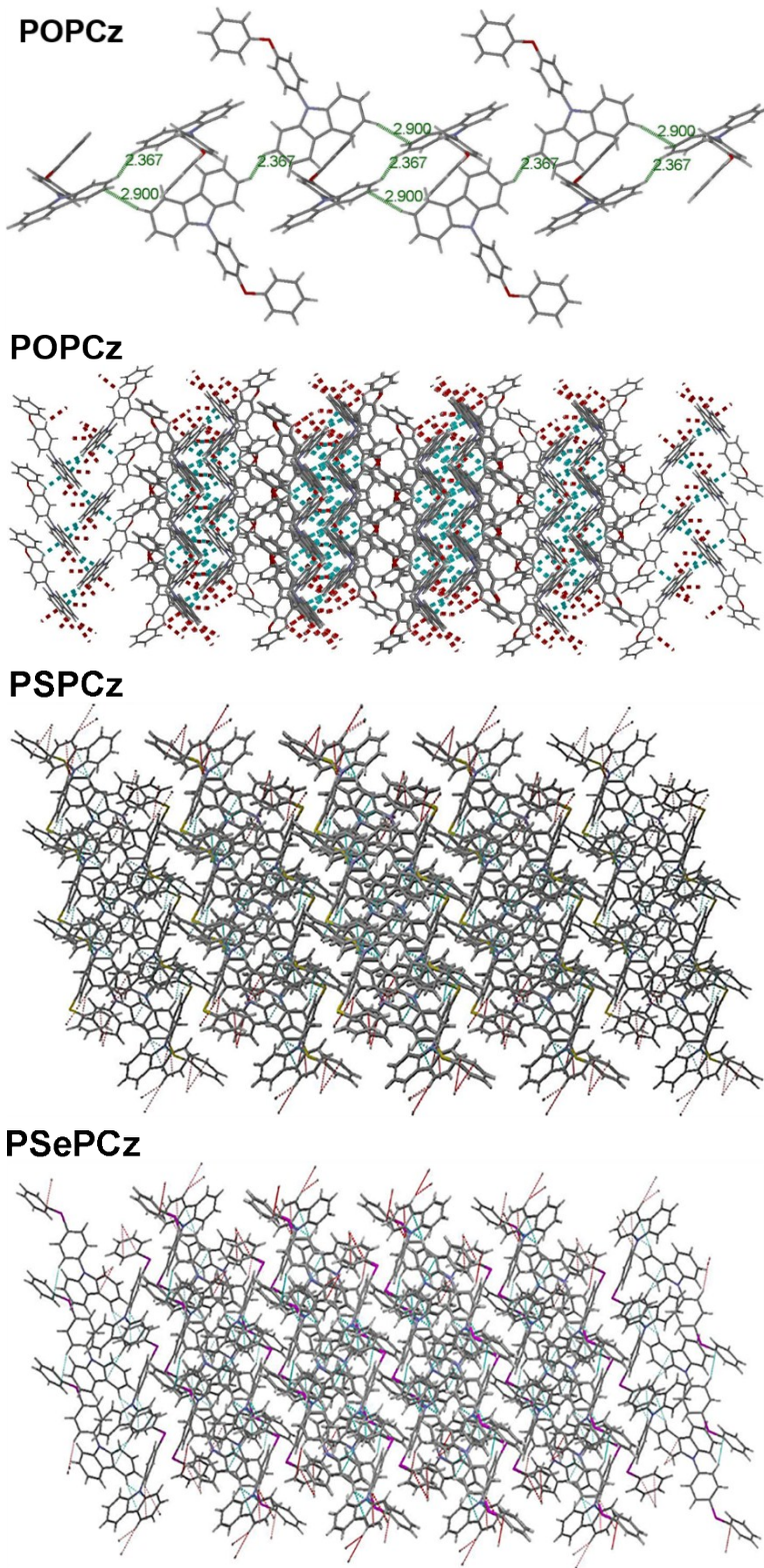
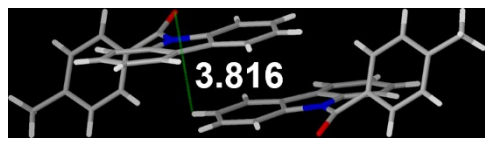
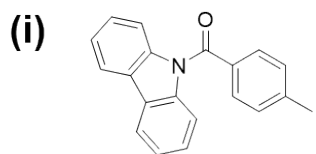
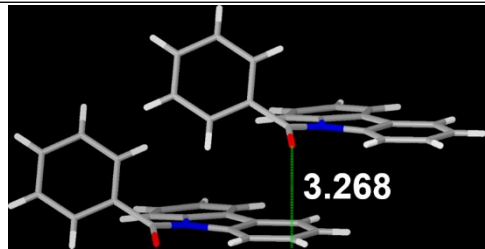
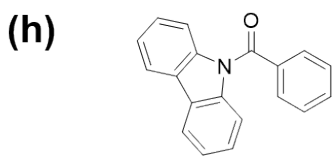
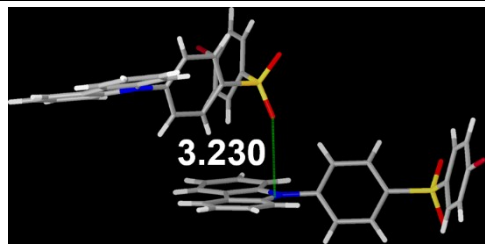
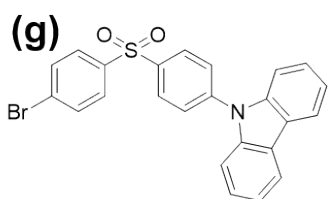
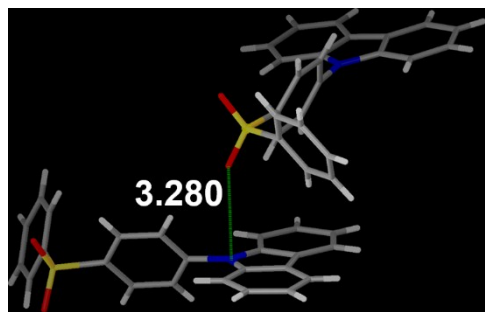
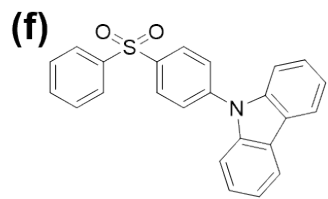
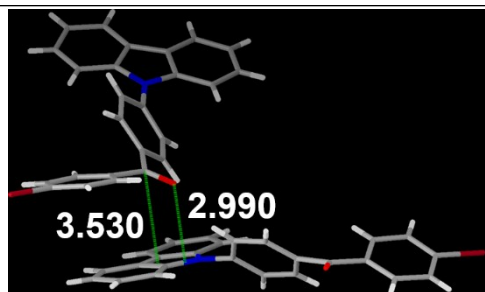
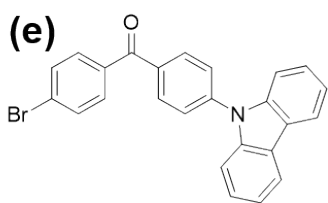


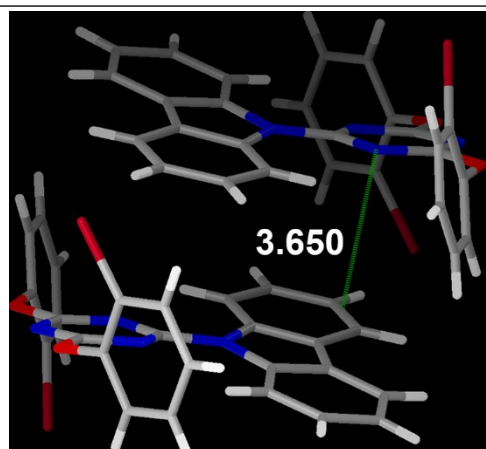
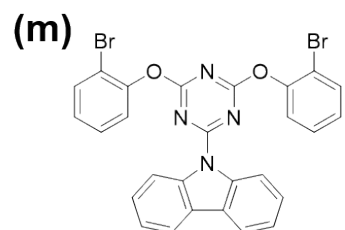
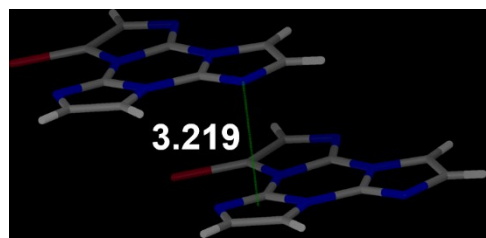
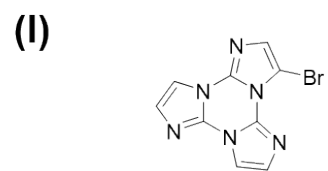
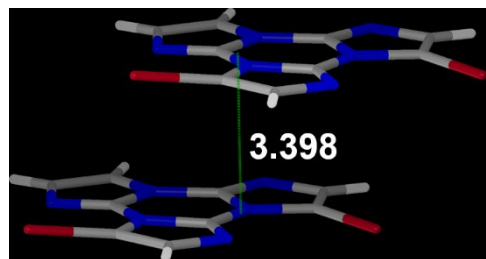
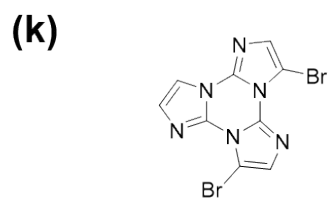
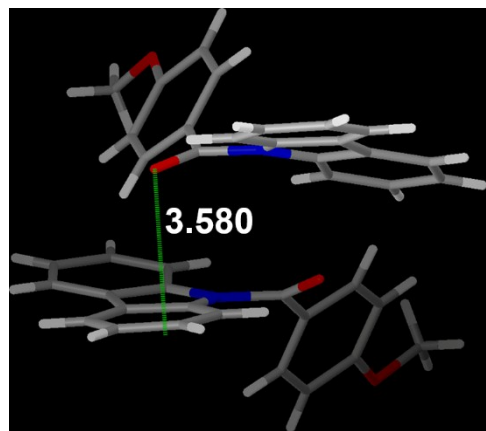
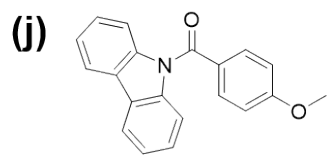
Fig. S27 Similar molecular packing of **POPCz**, **PSPCz** and **PSePCz** in crystal.

15. The distances of the n and π groups of some pRTP molecules in literature

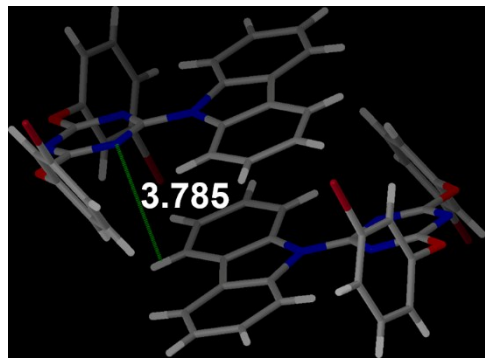
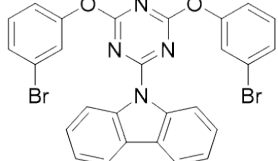
Table S6. The distances of intermolecular coupling of the n and π groups in two molecules that are adjacent in the single crystal of different compounds from literature references.

Molecular formulas	n and π distances (\AA)
(a)	
(b)	
(c)	
(d)	

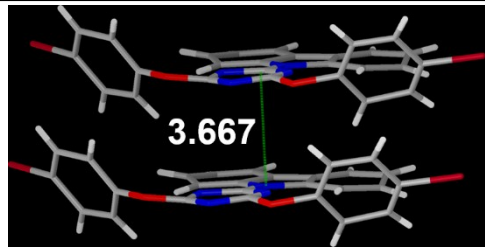
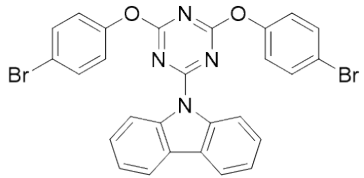




(n)



(o)



The distance from the n group to the coupled π plane of (a) CBA,⁴ (b) 4,4'-di(*N*-carbazolyl) benzophenone,⁵ (c) DPhCzT,⁶ (d) Cz-BP, (e) BCz-BP, (f) Cz-DPS, (g) BCz-DPS,⁷ (h) CPM, (i) CMPM,⁸ (j) CMOPM,⁸ (k) 3,7-dibromotriimidazo[1,2-a:1',2'-c:1'',2''-e] [1,3,5] triazine, (l) 3-bromotriimidazo[1,2-a:1',2'-c:1'',2''-e] [1,3,5] triazine,⁹ (m) o-BrTCz, (n) m-BrTCz, (o) p-BrTCz.¹⁰

(o)

p-BrTCz.¹⁰

16. Computational methods and results

The molecular geometries of ground states were obtained from the single crystal structures (**PEPCz**, E= O, S, Se) and optimized using the PBE0 functional (**PEPCz**, the structural optimization of **PTePCz** is based on the crystal structure of **POPCz**, **PSPCz** and **PSePCz**). A LANL08(d) basis set was employed for the Te atom and a 6-311G(d,p) basis set for the remaining atoms. The structures of all stationary points were fully optimized, and frequency calculations were performed at the same level. The frequency calculations confirmed the nature of all revealed equilibrium geometries: there were no imaginary frequencies. The vertical excitation energies and corresponding oscillator strengths of the first ten excited states of the n-th singlet (S_n) and n-th triplet states (T_n) were obtained on the corresponding ground state structure using the combination of TD-PBE0/6-311G** (LANL08(d) for the Te atom).

The molecular geometries of T_1 were optimized using the Δ SCF approach. The nature transition orbitals (NTOs) were calculated for S_1 and T_n states at optimized T_1 geometric structure using the TD-DFT method. For simplicity and clarity purpose, we calculated the dominant contributions and the associated weights (>85%) for the triplet states. The results are calculated by Gaussian 09 package.¹¹ The Multiwfn package^{12,13} is employed to calculate the components of n orbits based on Mulliken population analysis (MPA). The spin-orbit coupling (SOC) matrix elements between singlet and involved triplet states are given by Beijing Density Function (BDF) program^{14,15} using the cc-pVTZ-DK basis set. The calculated configuration proportion (α_n) of $^3(n, \pi^*)$ states and SOC are shown in Figure S30.

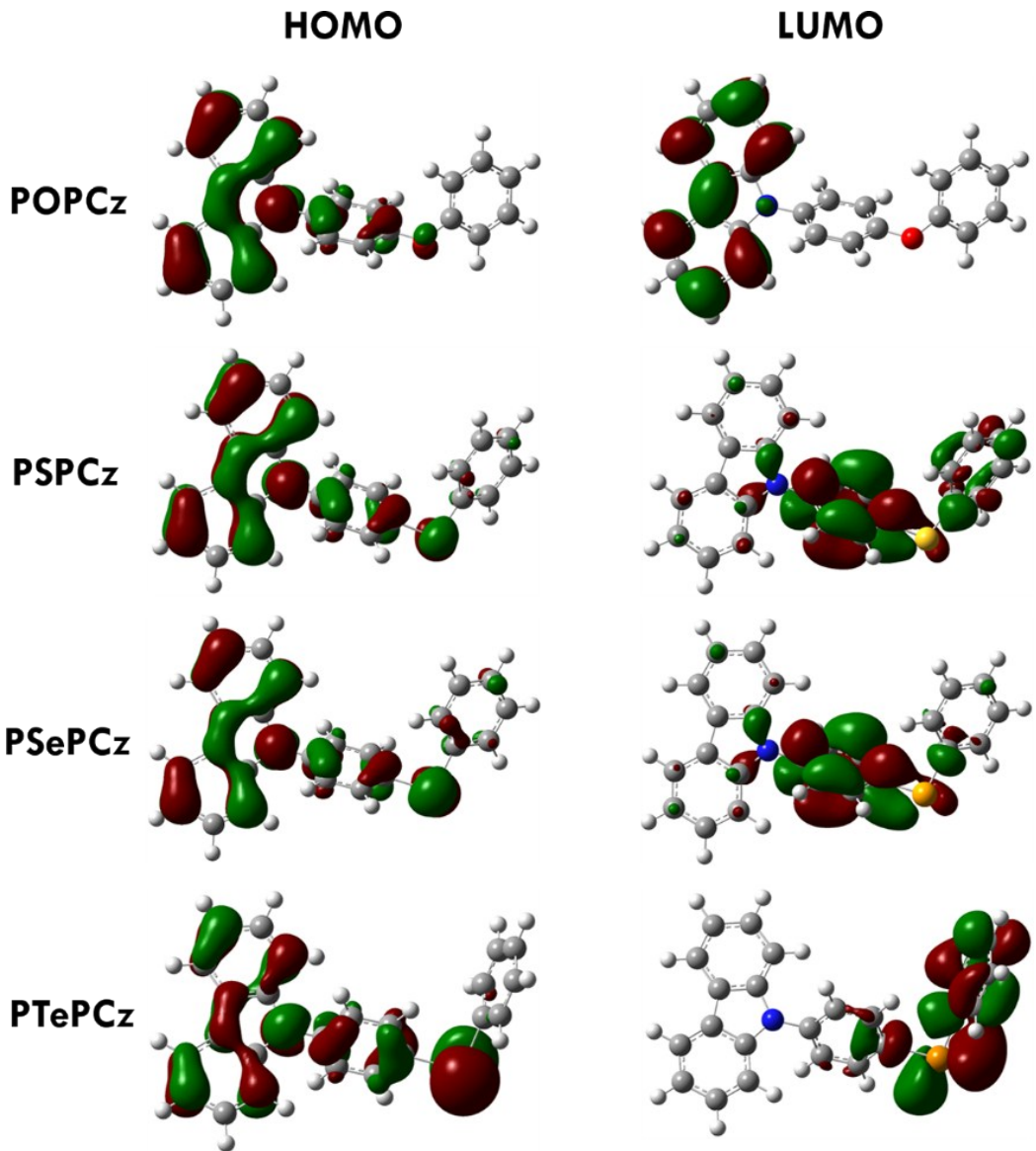


Fig. S28 Electrical density contour of HOMO and LUMO of **PEPCz** in gas phase (contour level=0.02).

Table S7. The singlet and triplet excited states transition configurations of **PEPCz** revealed by TD-DFT calculations. The matched excited states that contain the same orbital transition components of S_1 and T_1 were highlighted in red. Note that H and L refer to highest occupied molecular orbital (HOMO) and lowest unoccupied molecular orbital (LUMO), respectively.

		Transition configuration (%)
POPCz	S_1	H→L (89.60), H-1→L+5 (7.07)
	T_1	H→L (91.40), H-2→L (2.67), H-3→L+5 (2.48)
PSPCz	S_1	H→L (95.64)
	T_1	H→L (58.76), H-5→L (2.29), H-2→L (6.92), H-2→L+1 (3.30), H→L+1 (15.2)
PSePCz	S_1	H→L (90.26), H-1→L (6.08)
	T_1	H→L (62.69), H-1→L (3.87), H-5→L (4.44), H-1→L+1 (3.75), H→L+1 (13.88)
PTePCz	S_1	H→L (64.66), H-1→L (31.06)
	T_1	H→L (49.76), H-1→L (35.36), H-1→L+5 (3.03), H→L+2 (3.88)

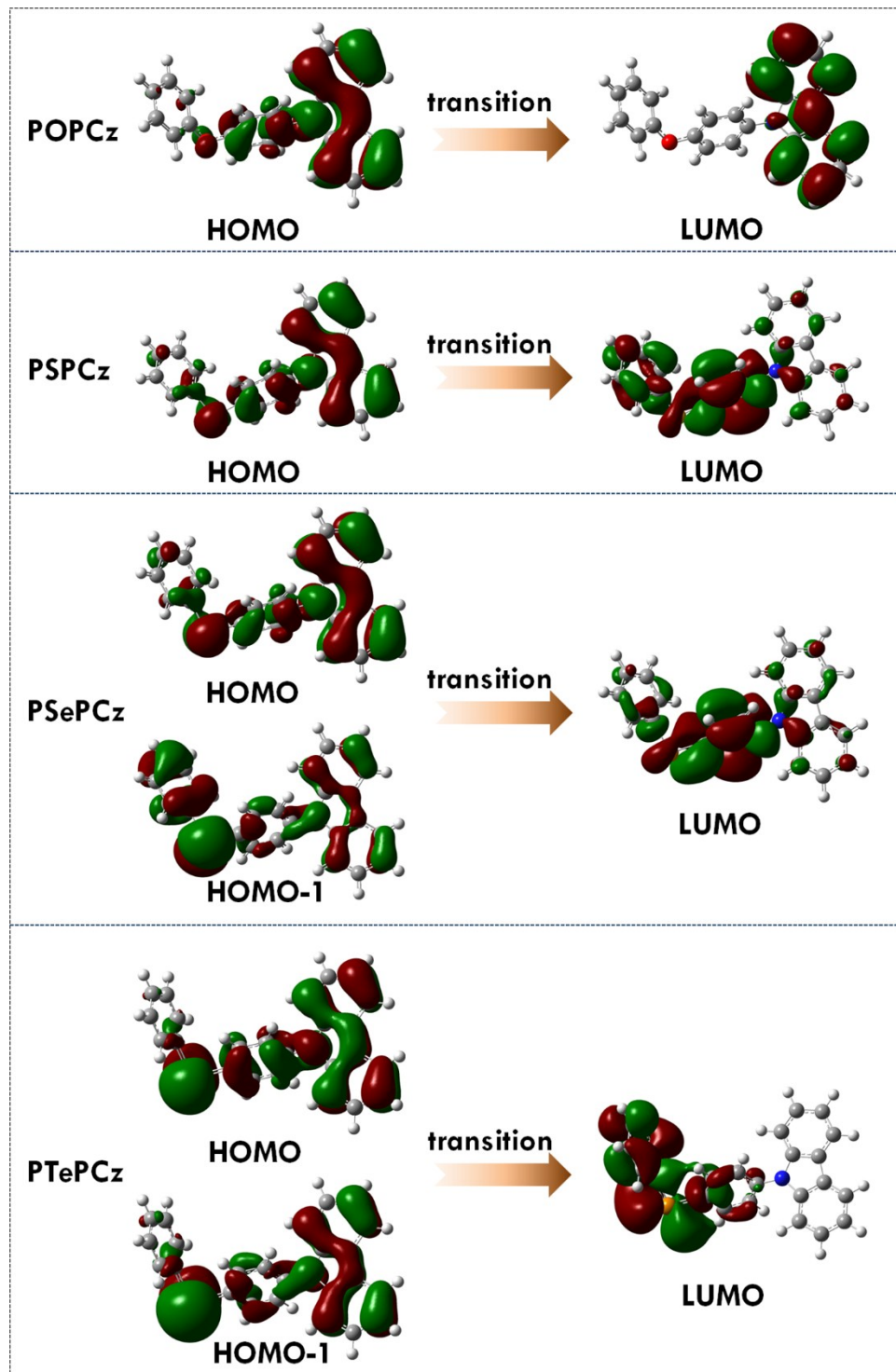


Fig. S29 The isosurface and main orbitals of transition configurations of **PEPCz** at S_1 and T_1 states.

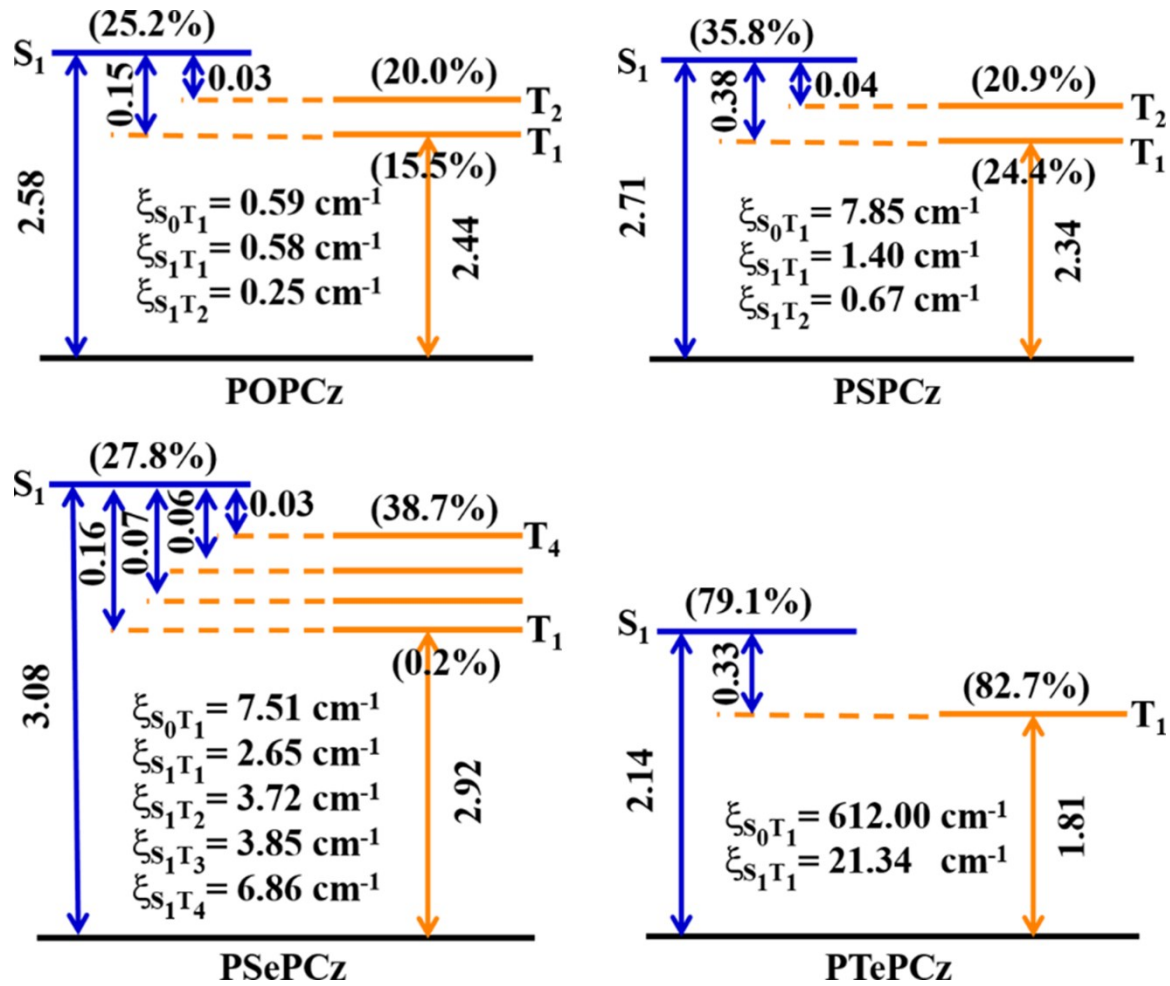


Fig. S30 Calculated energy diagram, ${}^3(n, \pi^*)$ configuration proportion (α_n) of S_1 and T_n , spin-orbit coupling (ξ) for the involved S_n and T_n states of PEPCz.

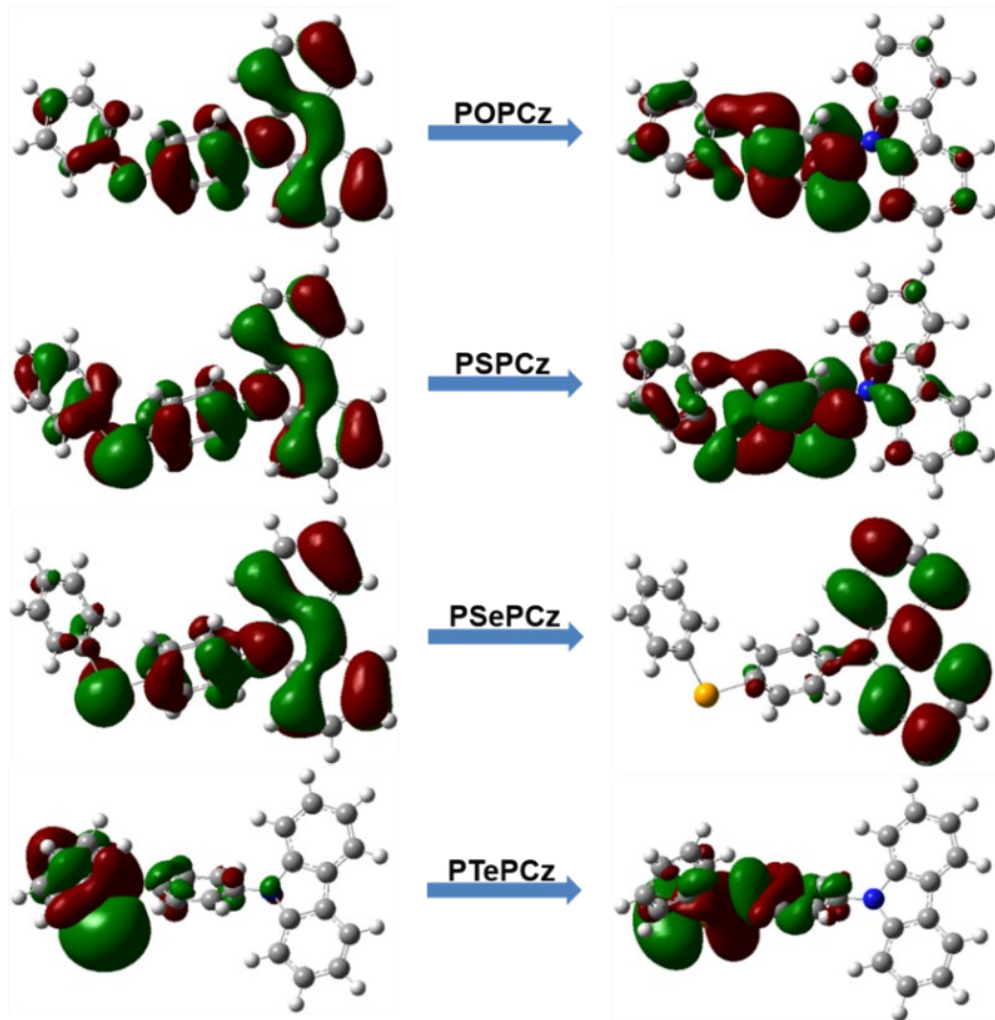


Fig. S31 The NTOs of S_1 states at optimized T_1 geometric structure.

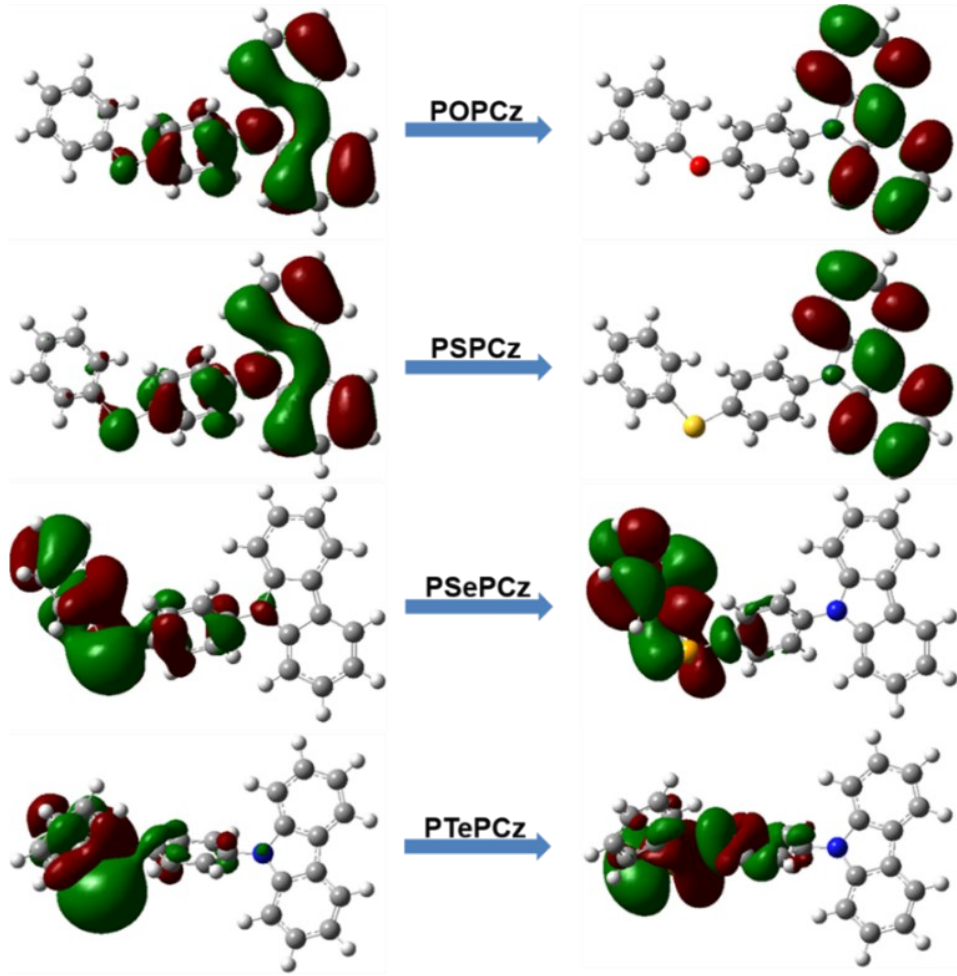


Fig. S32 The NTOs of T_n states ($n = 2$ for **POPCz** and **PSPCz**, $n = 4$ for **PSePCz** and $n = 1$ for **PTePCz**) at optimized T_1 geometric structure.

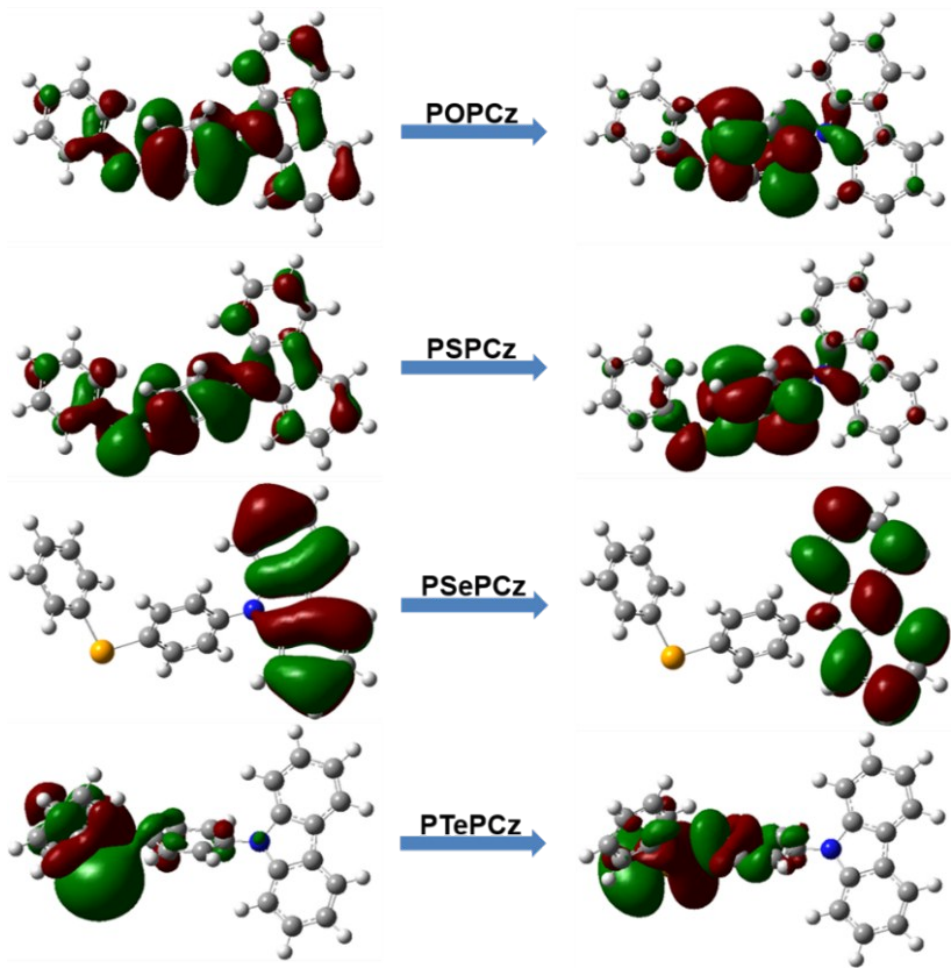


Fig. S33 The NTOs of T_1 states at optimized T_1 geometric structure.

17. Color-encryption application

Based on **PEPCz** unique pRTP properties, the molecules could be used in security protection with color-decryption^{16,17} and time-resolved⁷ features. The pRTP of **PEPCz** were affected by the different factors. This process like the changing of Chinese “Taiji”. We combined organic materials and inorganic materials (rare earth materials) in “Taiji” simultaneously. As shown in Fig.5a, under 365 nm UV irradiation, the transient emission of the “taiji” were enormous differences while the blue **PSPCz** part (right), Pink **PSePCz** part (left), red Eu(1,10-Phen)₂(NO₃)₃ part (upper circle) and green Tb(Salicylic Acid)₄(NO₃)₃ (lower circle) were observed. The “taiji” pattern demonstrate the advantages of pRTP of **PSPCz** and **PSePCz**. These compounds could distinguish by naked eyes hardly under daylight. Once the excitation was removed, only the **PSPCz** and **PSePCz** crystalline sample (orange) of “taiji” could clearly observed. After 2s, there is only **PSePCz** could be seen in the pattern. The changed pattern was observed as a result of the intrinsic emission differences between PL and pRTP, and distinctive pRTP performances of different **PEPCz** molecules. The entire pathway is exhibiting color-encryption and time-resolved dual-responsive security protection.

18. SEM of PSePCz aggregates in 50% volume fractions of EtOH in water

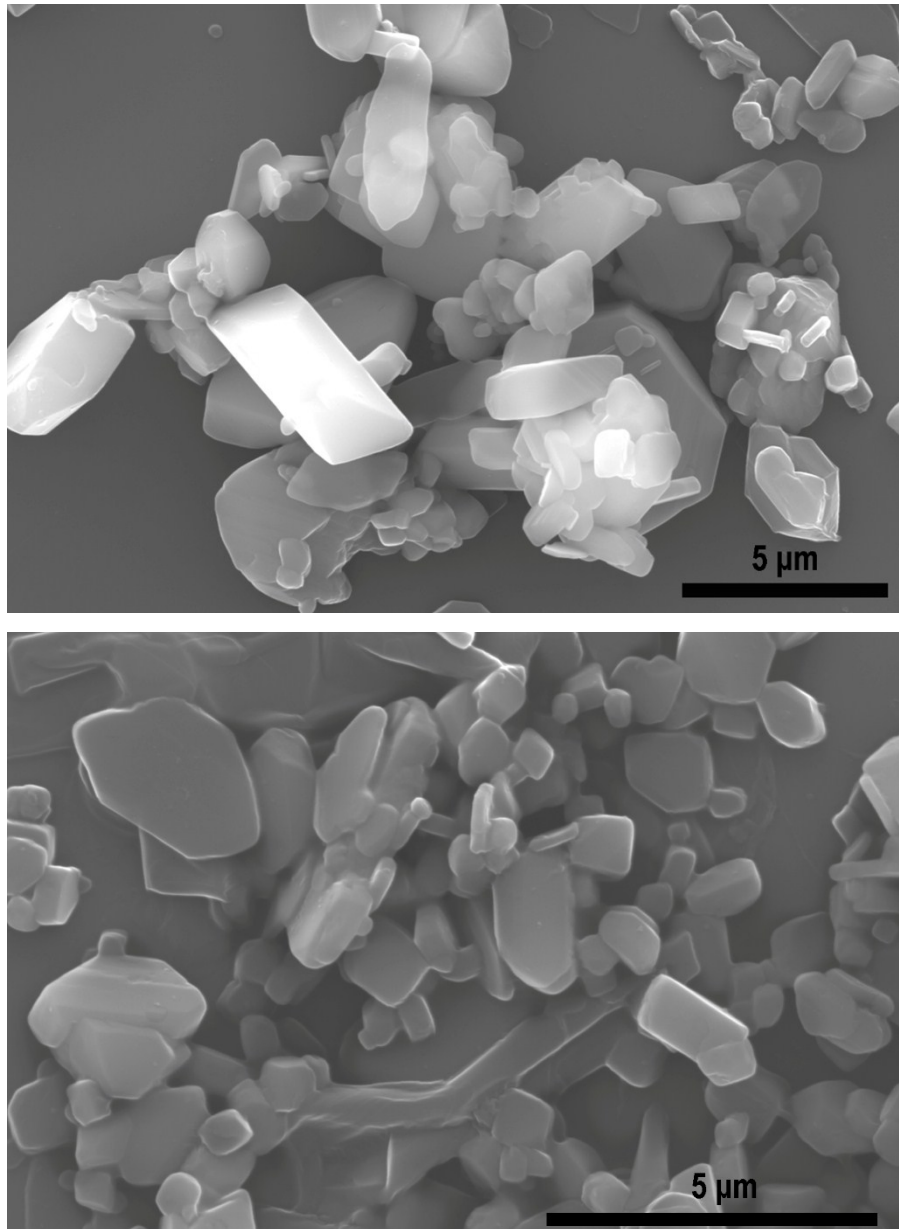


Fig. S34 SEM images of PSePCz aggregates obtained from a suspension containing 50% volume fraction of EtOH in water.

19. The pRTP sensing application details

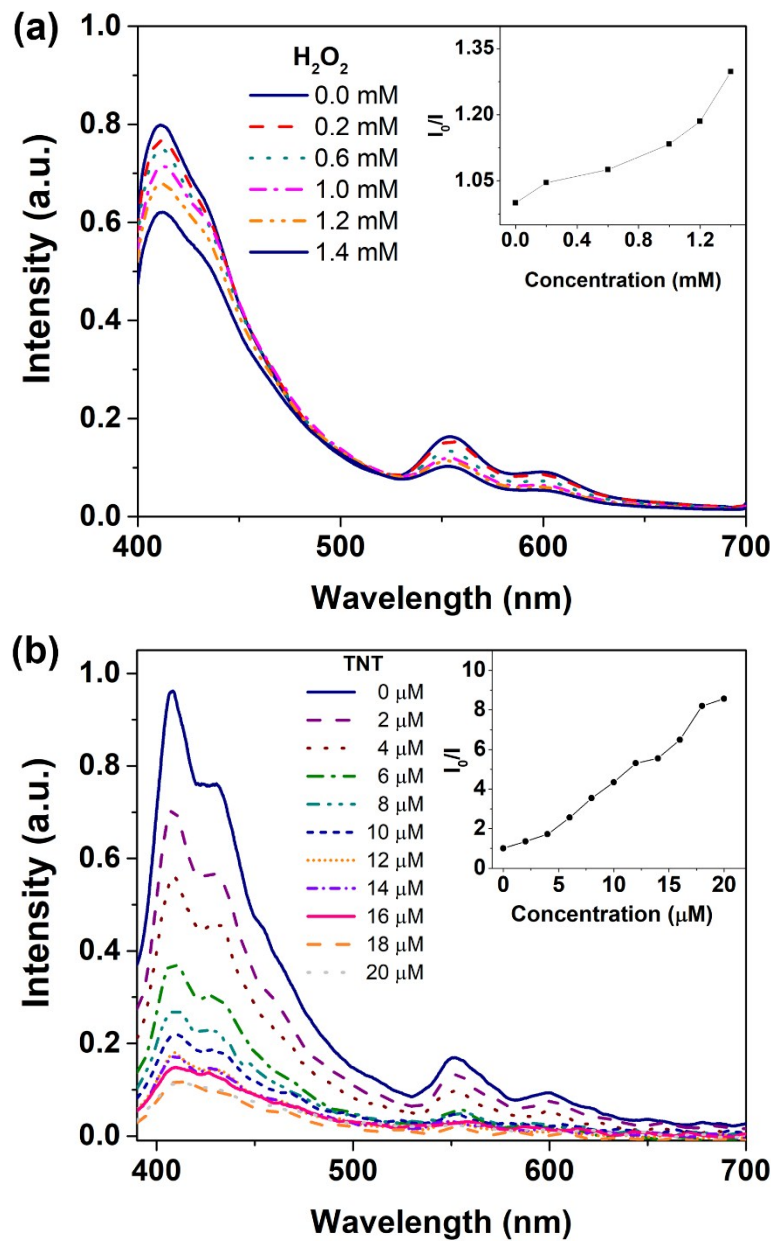


Fig. S35 Fluorescent sensing for H_2O_2 and TNT applications. (a) H_2O_2 and (b) TNT concentration-dependent fluorescence spectra of **PSePCz** aggregates in $\text{H}_2\text{O}/\text{EtOH}$ (50/50 v/v) solution. Inset: SternVolmer plots: fluorescence for H_2O_2 and TNT at different concentrations.

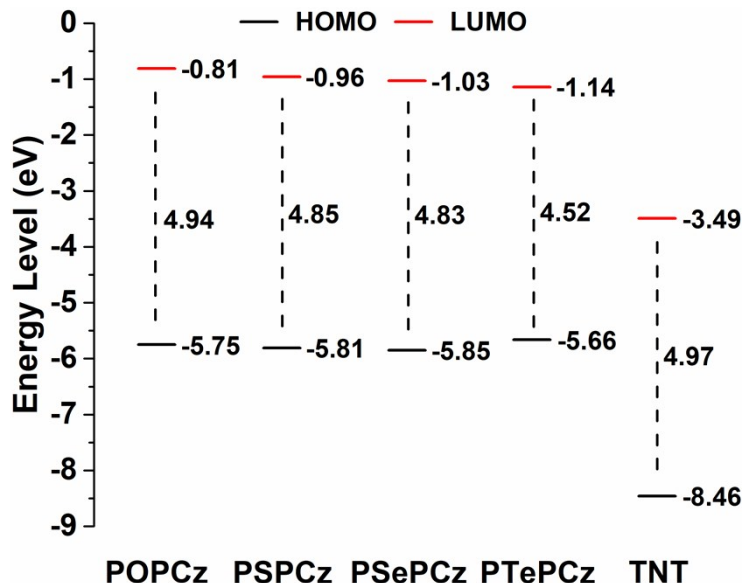


Fig. S36 Calculated orbital energy level of **PEPCz** and TNT.

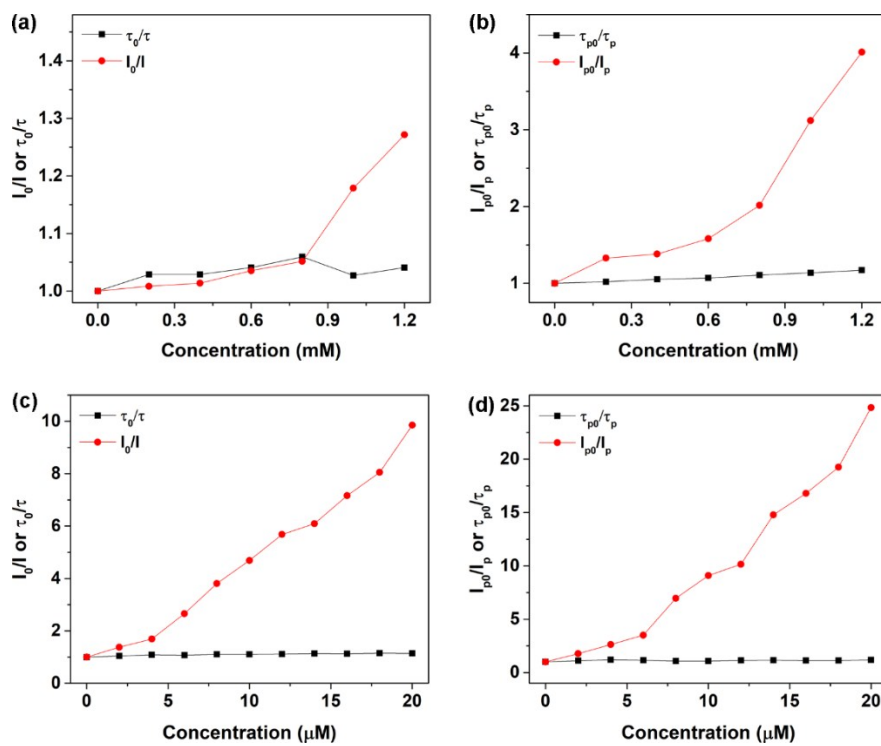


Fig. S37 For fluorescence, plots of the ratios of I_0/I and τ_0/τ of **PSePCz** aggregates against the concentration of (a) H_2O_2 and (c) TNT, respectively. For phosphorescence, plots of the ratios of I_{p0}/I_p and τ_{p0}/τ_p of **PSePCz** aggregates against the concentration of (b) H_2O_2 and (d) TNT, respectively.

20. The ^1H and ^{13}C NMR spectra of PEPCz in CDCl_3

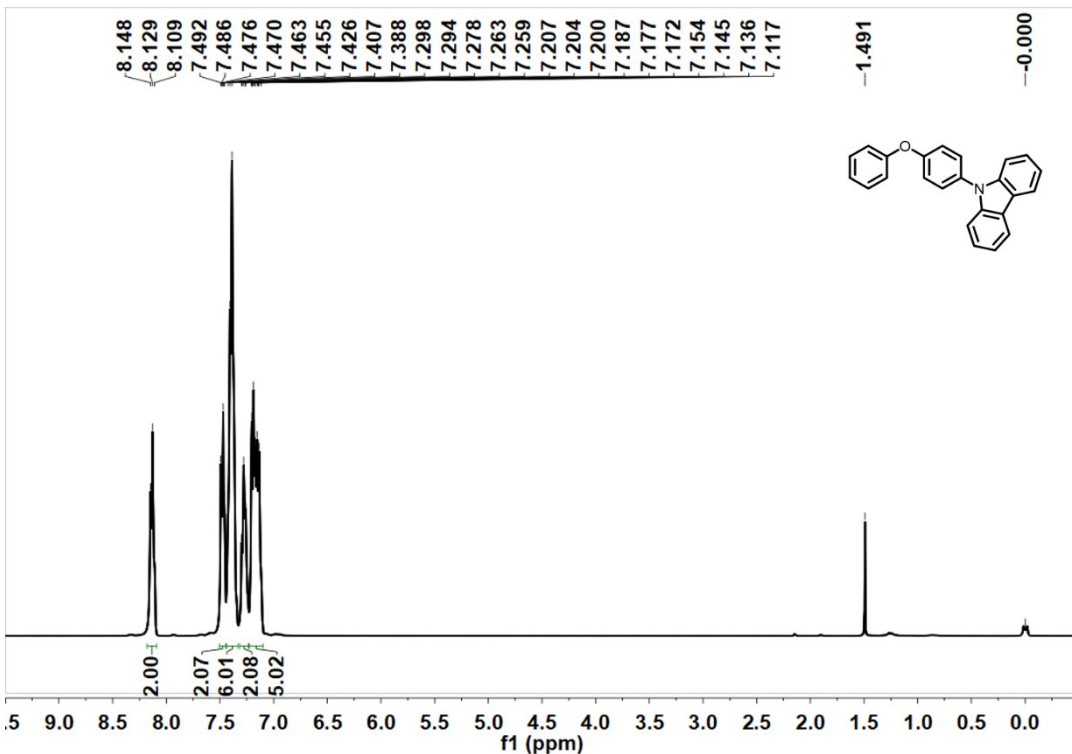


Fig. S38 The ^1H NMR spectrum of POPCz in CDCl_3 .

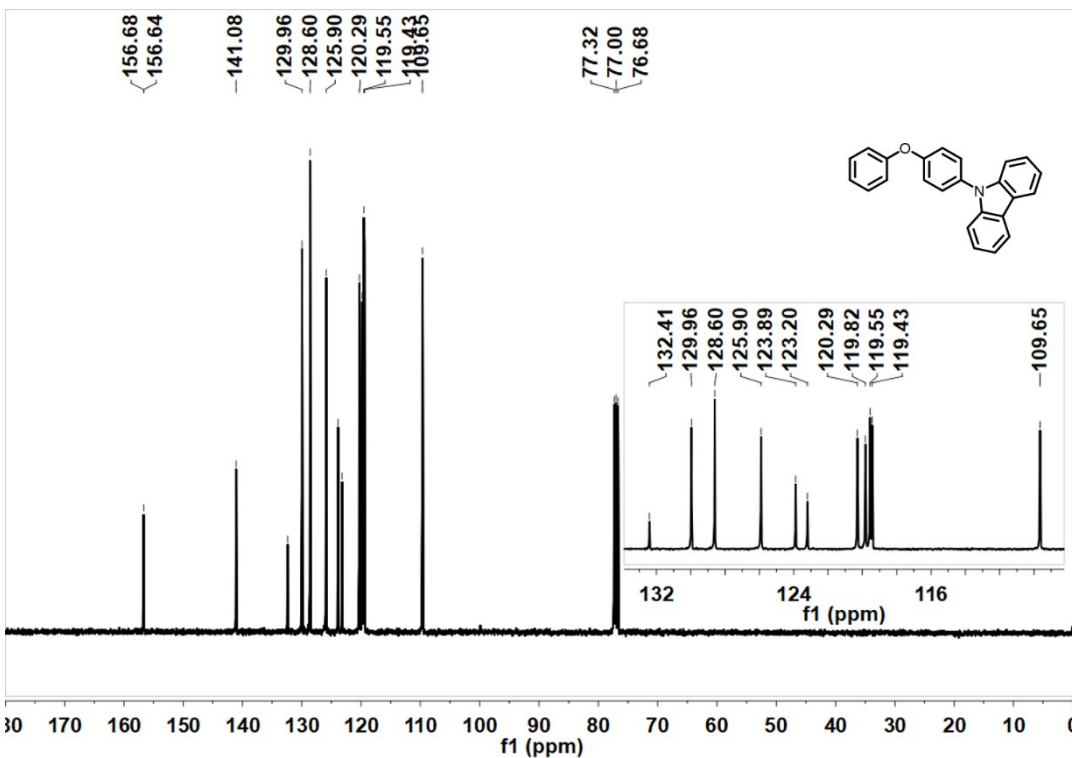


Fig. S39 The ^{13}C NMR spectrum of POPCz in CDCl_3 .

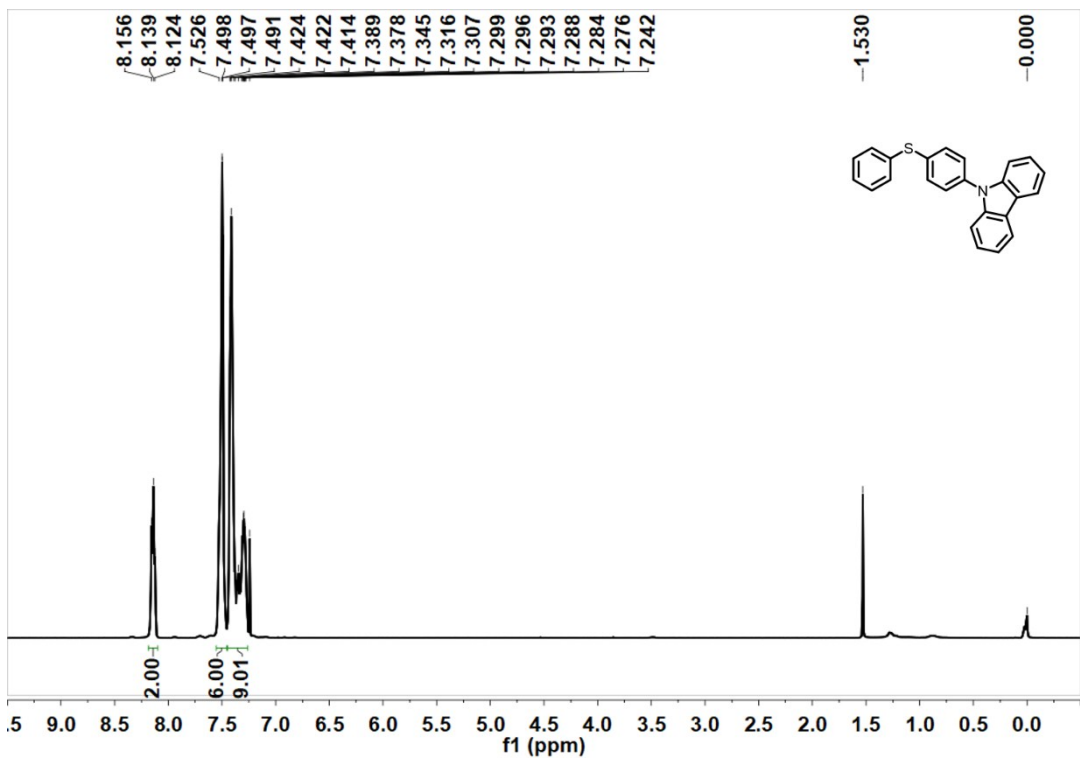


Fig. S40 The ^1H NMR spectrum of PSPCz in CDCl_3 .

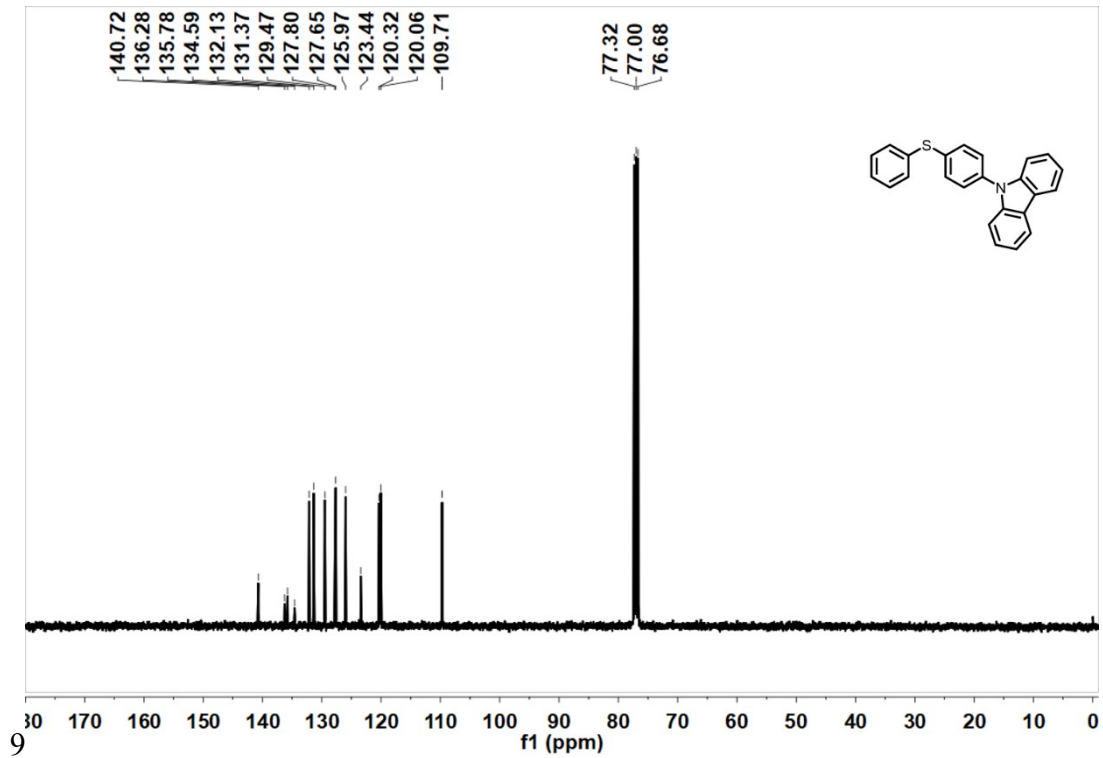


Fig. S41 The ^{13}C NMR spectrum of PSPCz in CDCl_3 .

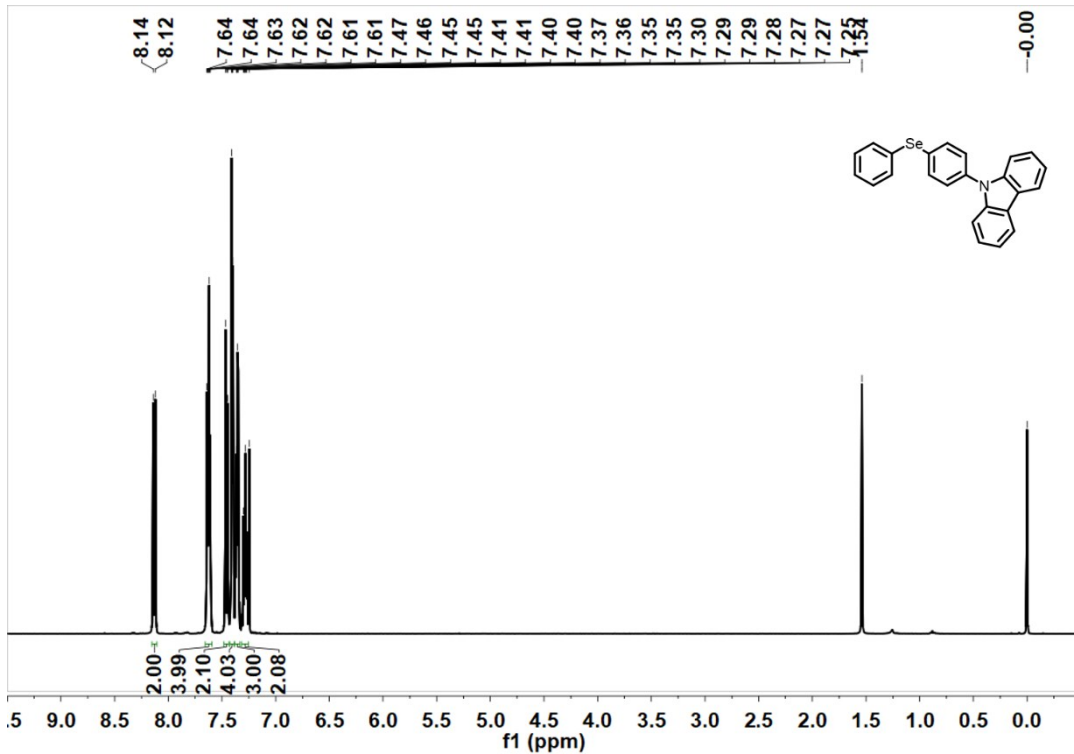


Fig. S42 The ^1H NMR spectrum of PSePCz in CDCl_3 .

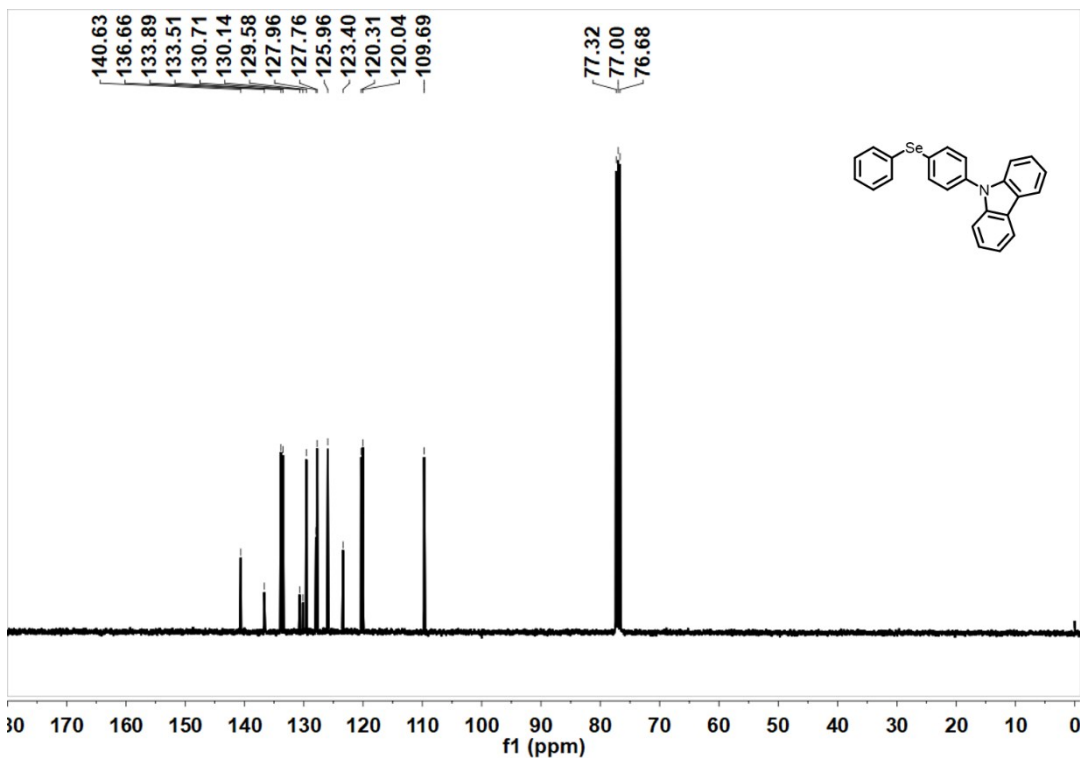


Fig. S43 The ^{13}C NMR spectrum of PSePCz in CDCl_3 .

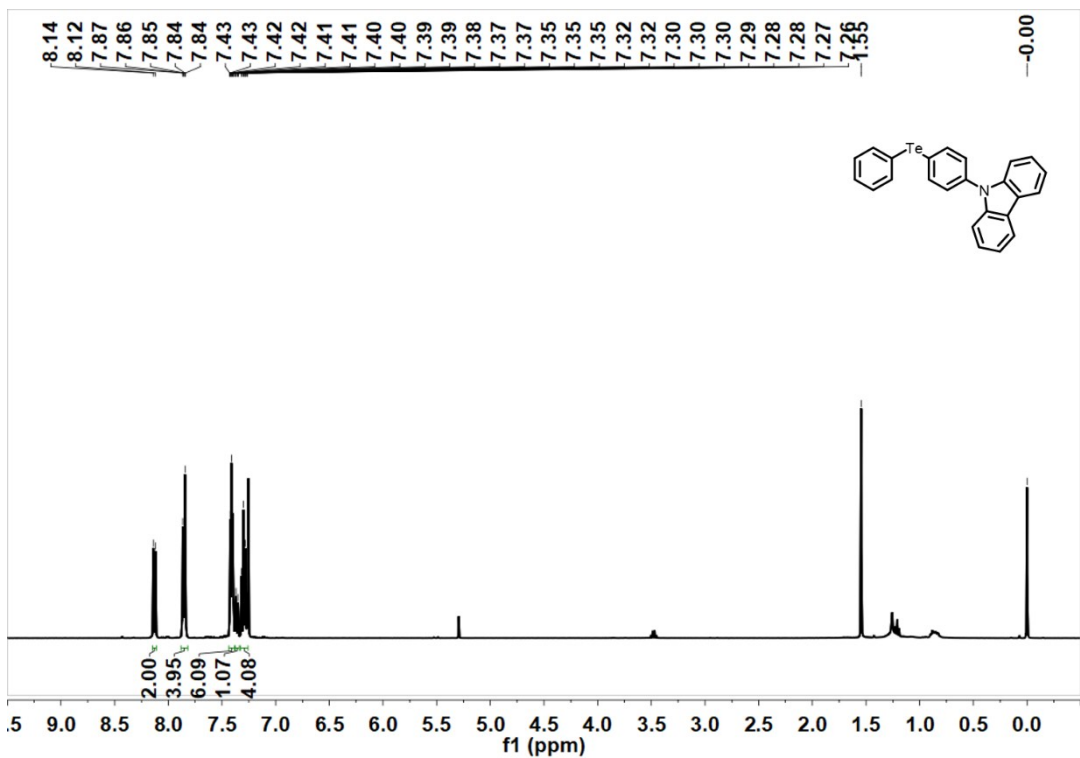


Fig. S44 The ^1H NMR spectrum of PTePCz in CDCl_3 .

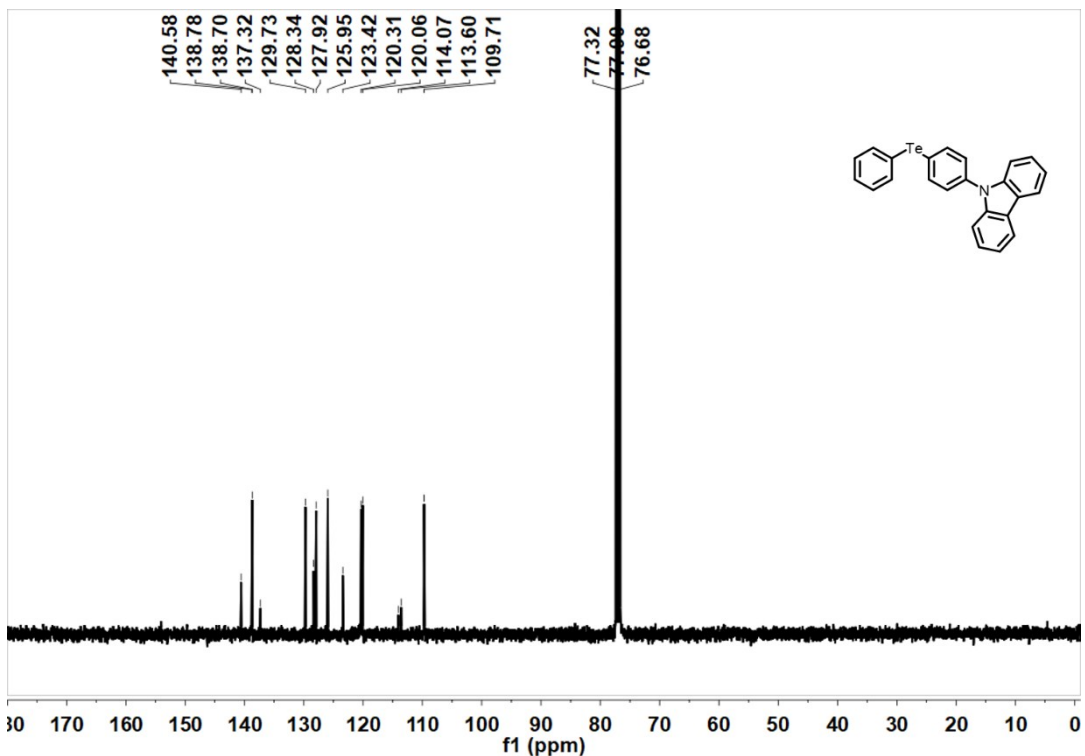


Fig. S45 The ^{13}C NMR spectrum of PTePCz in CDCl_3 .

21. Coordinates of molecular structures

Table S8. Cartesian coordinates of optimized geometry of **POPCz** (DFT, TD-PBE0/6-311G**) Standard orientation: (Ground State)

Center Number	Atomic Number	Atomic Type	Coordinates (Angstroms)		
			X	Y	Z
1	6	0	5.733370	1.638854	0.089956
2	1	0	5.775909	2.693376	0.341606
3	8	0	3.591060	-1.287182	0.647187
4	6	0	1.845607	-0.133231	-0.583914
5	1	0	2.555151	0.251714	-1.307028
6	6	0	0.490935	0.134180	-0.721151
7	1	0	0.136446	0.725712	-1.558284
8	6	0	-2.577553	3.552348	0.196688
9	1	0	-2.127329	4.532437	0.315266
10	6	0	0.023851	-1.149621	1.258686
11	1	0	-0.689339	-1.527696	1.982949
12	6	0	1.373038	-1.433402	1.393622
13	1	0	1.741167	-2.043108	2.210631
14	6	0	-2.724043	-2.404168	-0.185048
15	1	0	-1.766812	-2.909477	-0.125603
16	6	0	-3.901444	-3.115781	-0.358582
17	1	0	-3.858810	-4.197664	-0.429326
18	6	0	4.650683	0.880415	0.514834
19	1	0	3.851005	1.326508	1.095852
20	6	0	2.285591	-0.920355	0.476784
21	7	0	-1.804879	-0.078324	0.059336
22	6	0	-2.374757	1.187456	0.062688
23	6	0	-1.764573	2.429184	0.217602
24	1	0	-0.692741	2.514985	0.355304
25	6	0	-3.963570	3.448431	0.029763
26	1	0	-4.569114	4.348084	0.016755
27	6	0	-2.814945	-1.017618	-0.098384
28	6	0	-3.772360	1.062771	-0.095988
29	6	0	6.762322	1.054840	-0.641136
30	1	0	7.606618	1.652466	-0.966498
31	6	0	4.601118	-0.472158	0.192772
32	6	0	-0.427407	-0.364119	0.199338

33	6	0	-5.139996	-2.469396	-0.448146
34	1	0	-6.041158	-3.057692	-0.582488
35	6	0	-5.222380	-1.088470	-0.372102
36	1	0	-6.182725	-0.588978	-0.450235
37	6	0	-4.054027	-0.347843	-0.197626
38	6	0	-4.565980	2.208982	-0.113463
39	1	0	-5.641617	2.130296	-0.234604
40	6	0	5.622809	-1.067511	-0.534666
41	1	0	5.556646	-2.125617	-0.760759
42	6	0	6.704968	-0.299628	-0.946429
43	1	0	7.504836	-0.764580	-1.512968

Zero-point correction=	0.343425
Thermal correction to Energy=	0.362683
Thermal correction to Enthalpy=	0.363627
Thermal correction to Gibbs Free Energy=	0.292661
Sum of electronic and zero-point Energies=	-1053.44466
Sum of electronic and thermal Energies=	-1053.42540
Sum of electronic and thermal Enthalpies=	-1053.42446
Sum of electronic and thermal Free Energies=	-1053.49543

Table S9. Cartesian coordinates of optimized geometry of **PSPCz** (DFT, TD-PBE0/6-311G**) Standard orientation: (Ground State)

Center Number	Atomic Number	Atomic Type	Coordinates (Angstroms)		
			X	Y	Z
1	7	0	-1.978652	-0.087636	-0.001904
2	16	0	3.709323	-1.923786	0.148322
3	6	0	4.378491	0.684217	0.838084
4	1	0	3.531117	0.657071	1.514437
5	6	0	4.661670	-0.423272	0.038135
6	6	0	5.759035	-0.397130	-0.820077
7	1	0	5.969155	-1.256166	-1.448234
8	6	0	1.603300	-0.423131	-0.866982
9	1	0	2.303646	-0.053955	-1.608010
10	6	0	2.038719	-1.317011	0.112345
11	6	0	1.127881	-1.805308	1.046817
12	1	0	1.466378	-2.486298	1.820106
13	6	0	-0.200150	-1.401982	1.009549
14	1	0	-0.902237	-1.761727	1.753627
15	6	0	-0.631830	-0.504625	0.036107
16	6	0	6.571698	0.729784	-0.872179
17	1	0	7.426157	0.742547	-1.540763
18	6	0	6.282015	1.838862	-0.088396
19	1	0	6.911140	2.721045	-0.138232
20	6	0	5.180319	1.813501	0.761534
21	1	0	4.951873	2.674301	1.381509
22	6	0	-2.420180	1.230758	0.015023
23	6	0	-1.683837	2.409029	0.104294
24	1	0	-0.601893	2.394309	0.165956
25	6	0	-3.830580	1.242427	-0.035094
26	6	0	-3.087698	-0.924474	-0.062018
27	6	0	-3.144742	-2.313617	-0.134379
28	1	0	-2.243245	-2.915152	-0.142199
29	6	0	0.279548	-0.018256	-0.902870
30	1	0	-0.063803	0.659549	-1.676723
31	6	0	-4.397839	-2.903181	-0.207555
32	1	0	-4.469339	-3.984304	-0.264292
33	6	0	-5.568034	-2.135415	-0.214342
34	1	0	-6.531507	-2.630090	-0.270605

35	6	0	-5.504125	-0.752745	-0.157485
36	1	0	-6.411641	-0.157840	-0.174489
37	6	0	-4.256958	-0.134287	-0.083629
38	6	0	-4.509535	2.459820	-0.016552
39	1	0	-5.593799	2.484148	-0.055083
40	6	0	-3.781666	3.636332	0.056331
41	1	0	-4.296829	4.590580	0.069334
42	6	0	-2.383947	3.605992	0.120883
43	1	0	-1.833113	4.538299	0.188550

Zero-point correction=	0.340588
Thermal correction to Energy=	0.360518
Thermal correction to Enthalpy=	0.361462
Thermal correction to Gibbs Free Energy=	0.288963
Sum of electronic and zero-point Energies=	-1376.349291
Sum of electronic and thermal Energies=	-1376.329361
Sum of electronic and thermal Enthalpies=	-1376.328417
Sum of electronic and thermal Free Energies=	-1376.400915

Table S10. Cartesian coordinates of optimized geometry of **PSePCz** (DFT, TD-PBE0/6-311G**) Standard orientation: (Ground State)

Center Number	Atomic Number	Atomic Type	Coordinates (Angstroms)		
			X	Y	Z
1	7	0	-2.335561	-0.042732	-0.039882
2	34	0	3.555834	-1.689839	-0.081070
3	6	0	-0.472840	-1.262181	0.936555
4	1	0	-1.129505	-1.615789	1.723736
5	6	0	0.869415	-1.620332	0.928614
6	1	0	1.262700	-2.259976	1.711110
7	6	0	1.719872	-1.135967	-0.061980
8	6	0	1.213089	-0.296707	-1.053941
9	1	0	1.866285	0.066273	-1.839611
10	6	0	4.408522	0.026502	0.047301
11	6	0	3.867165	1.064794	0.802428
12	1	0	2.918219	0.930746	1.310034
13	6	0	4.547002	2.271705	0.900428
14	1	0	4.118256	3.079156	1.485242
15	6	0	-0.125364	0.062046	-1.047060
16	1	0	-0.525882	0.697543	-1.829280
17	6	0	-0.976298	-0.416840	-0.049357
18	6	0	-3.419811	-0.913301	-0.001148
19	6	0	-4.612421	-0.158824	0.005159
20	6	0	-4.227361	1.230429	-0.030593
21	6	0	-2.816820	1.262266	-0.057595
22	6	0	-2.114747	2.464562	-0.058878
23	1	0	-1.031182	2.485277	-0.055838
24	6	0	-2.850864	3.639908	-0.054732
25	1	0	-2.327006	4.590026	-0.056998
26	6	0	-4.250206	3.626298	-0.043756
27	1	0	-4.793986	4.564606	-0.042889
28	6	0	-4.942970	2.426729	-0.026815
29	1	0	-6.027941	2.417063	-0.006568
30	6	0	-5.842034	-0.815156	0.025857
31	1	0	-6.767015	-0.247586	0.030787
32	6	0	-4.674152	-2.933184	0.012402
33	1	0	-4.715021	-4.017350	0.007677
34	6	0	-3.437730	-2.305386	-0.008509

35	1	0	-2.520162	-2.881354	-0.038940
36	6	0	-5.866163	-2.200235	0.034424
37	1	0	-6.815530	-2.724167	0.052211
38	6	0	5.633261	0.197433	-0.594820
39	1	0	6.047857	-0.604733	-1.196737
40	6	0	6.316402	1.401828	-0.472995
41	1	0	7.270504	1.527922	-0.974322
42	6	0	5.774351	2.443584	0.269260
43	1	0	6.304179	3.386180	0.354450

Zero-point correction= 0.339415
 Thermal correction to Energy= 0.359814
 Thermal correction to Enthalpy= 0.360759
 Thermal correction to Gibbs Free Energy= 0.286248
 Sum of electronic and zero-point Energies= -3379.517024
 Sum of electronic and thermal Energies= -3379.496625
 Sum of electronic and thermal Enthalpies= -3379.495681
 Sum of electronic and thermal Free Energies= -3379.570192

Table S11. Cartesian coordinates of optimized geometry of **PTePCz** (DFT, TD-PBE0/ LANL08(d) + 6-311G**) Standard orientation: (Ground State)

Center Number	Atomic Number	Atomic Type	Coordinates (Angstroms)		
			X	Y	Z
1	7	0	-2.688429	-0.006362	0.024498
2	6	0	-0.873701	-1.305524	0.992087
3	1	0	-1.592112	-1.818561	1.622340
4	6	0	0.477866	-1.608775	1.079277
5	1	0	0.804079	-2.365079	1.786658
6	6	0	1.407124	-0.927769	0.293240
7	6	0	0.964546	0.061493	-0.583211
8	1	0	1.672657	0.595783	-1.207578
9	6	0	4.231643	0.409369	-0.169235
10	6	0	4.171104	1.505189	0.693208
11	1	0	3.714935	1.399669	1.671438
12	6	0	4.694167	2.729644	0.296553
13	1	0	4.639901	3.579883	0.968683
14	6	0	-0.386898	0.363321	-0.672691
15	1	0	-0.732637	1.119805	-1.369098
16	6	0	-1.314208	-0.317797	0.113862
17	6	0	-3.706602	-0.905301	-0.268784
18	6	0	-4.940362	-0.219242	-0.262888
19	6	0	-4.648631	1.158145	0.048615
20	6	0	-3.250212	1.249511	0.219173
21	6	0	-2.633691	2.449658	0.562836
22	1	0	-1.561870	2.509064	0.712859
23	6	0	-3.440786	3.566893	0.715680
24	1	0	-2.984795	4.514508	0.982834
25	6	0	-4.827341	3.497340	0.537193
26	1	0	-5.428031	4.391506	0.663098
27	6	0	-5.436436	2.297233	0.208395
28	1	0	-6.512754	2.242644	0.080475
29	6	0	-6.115002	-0.914932	-0.545713
30	1	0	-7.070997	-0.401239	-0.545043
31	6	0	-4.810770	-2.930006	-0.846861
32	1	0	-4.776323	-3.988226	-1.083972
33	6	0	-3.627424	-2.262479	-0.569285
34	1	0	-2.674796	-2.778934	-0.593812

35	6	0	-6.044279	-2.268536	-0.832158
36	1	0	-6.950357	-2.822273	-1.052613
37	6	0	4.832861	0.545305	-1.420403
38	1	0	4.877378	-0.302891	-2.095016
39	6	0	5.367343	1.770866	-1.805732
40	1	0	5.835009	1.870519	-2.779833
41	6	0	5.295372	2.862919	-0.950517
42	1	0	5.709304	3.818784	-1.254079
43	52	0	3.452621	-1.468454	0.429333

Zero-point correction= 0.338460
 Thermal correction to Energy= 0.359271
 Thermal correction to Enthalpy= 0.360215
 Thermal correction to Gibbs Free Energy= 0.283458
 Sum of electronic and zero-point Energies= -986.337128
 Sum of electronic and thermal Energies= -986.316317
 Sum of electronic and thermal Enthalpies= -986.315373
 Sum of electronic and thermal Free Energies= -986.392130

Reference

- (1) Kumar, A.; Bhakuni, B. S.; Prasad, C. D.; Kumar, S.; Kumar, S. *Tetrahedron* **2013**, *69*, 5383.
- (2) Kumar, A.; Kumar, S. *Tetrahedron* **2014**, *70*, 1763.
- (3) Yu, F.; Li, P.; Wang, B.; Han, K. *J. Am. Chem. Soc.* **2013**, *135*, 7674.
- (4) Xue, P.; Sun, J.; Chen, P.; Wang, P.; Yao, B.; Gong, P.; Zhang, Z.; Lu, R. *Chem. Commun.* **2015**, *51*, 10381.
- (5) Li, C.; Tang, X.; Zhang, L.; Li, C.; Liu, Z.; Bo, Z.; Dong, Y. Q.; Tian, Y. H.; Dong, Y.; Tang, B. Z. *Adv. Opt. Mater.* **2015**, *3*, 1184.
- (6) An, Z.; Zheng, C.; Tao, Y.; Chen, R.; Shi, H.; Chen, T.; Wang, Z.; Li, H.; Deng, R.; Liu, X.; Huang, W. *Nat. Mater.* **2015**, *14*, 685.
- (7) Yang, Z.; Mao, Z.; Zhang, X.; Ou, D.; Mu, Y.; Zhang, Y.; Zhao, C.; Liu, S.; Chi, Z.; Xu, J.; Wu, Y. C.; Lu, P. Y.; Lien, A.; Bryce, M. R. *Angew. Chem., Int. Ed.* **2016**, *55*, 2181.
- (8) Xie, Y.; Ge, Y.; Peng, Q.; Li, C.; Li, Q.; Li, Z. *Adv. Mater.* **2017**, *29*, 1606829.
- (9) Lucenti, E.; Forni, A.; Botta, C.; Carlucci, L.; Giannini, C.; Marinotto, D.; Pavanello, A.; Previtali, A.; Righetto, S.; Cariati, E. *Angew. Chem., Int. Ed.* **2017**, *56*, 16302.
- (10) Cai, S.; Shi, H.; Tian, D.; Ma, H.; Cheng, Z.; Wu, Q.; Gu, M.; Huang, L.; An, Z.; Peng, Q.; Huang, W. *Adv. Funct. Mater.* **2018**, 1705045.
- (11) Frisch, M.; Trucks, G.; Schlegel, H. B.; Scuseria, G.; Robb, M.; Cheeseman, J.; Scalmani, G.; Barone, V.; Mennucci, B.; Petersson, G. *Inc., Wallingford, CT* **2009**, 200.
- (12) Lu, T.; Chen, F. *J. Comput. Chem.* **2012**, *33*, 580.
- (13) Lu, T. C. *Acta Chim. Sinica* **2011**, *20*, 2393.
- (14) Liu, W. J.; Hong, G. Y.; Dai, D. D.; Li, L. M.; Dolg, M. *Theor. Chem. Acc.* **1997**, *96*, 75.
- (15) Liu, W. J.; Wang, F.; Li, L. M. *J. Theor. Comput. Chem.* **2003**, *2*, 257.
- (16) Xue, J.; Zhou, Z. K.; Wei, Z.; Su, R.; Lai, J.; Li, J.; Li, C.; Zhang, T.; Wang, X. H. *Nat. Commun.* **2015**, *6*, 8906.
- (17) Burgess, I. B.; Mishchenko, L.; Hatton, B. D.; Kolle, M.; Loncar, M.; Aizenberg, J. *J. Am. Chem. Soc.* **2011**, *133*, 12430.